Journal of Materials Chemistry B

ROYAL SOCIETY OF CHEMISTRY

REVIEW

View Article Online
View Journal | View Issue

Cite this: J. Mater. Chem. B, 2023, 11, 5350

Ultrasound nanomedicine and materdicine

Zeyu Wang,†[a] Xue Wang,†[d] Meiqi Chang,*[b] Jia Guo *[c] and Yu Chen *[a]

The conventional microbubble-based ultrasound biomedicine clinically plays a vital role in providing the dynamic detection of macro and microvasculature and disease theranostics. However, the intrinsic limitation of particle size severely decreases the treatment effectiveness due to their vascular transport characteristics, which promotes the development and application of multifunctional ultrasound-responsive nanomaterials. Herein, we put forward a research field of "ultrasound nanomedicine and materdicine", referring to the interdiscipline of ultrasound, nanobiotechnology and materials, which seeks to produce specific biological effects for addressing the challenges faced and dilemma of conventional ultrasound medicine. We comprehensively summarize the state-of-the-art scientific advances in the latest progress in constructing ultrasound-based platforms and ultrasound-activated sonosensitizers, ranging from the synthesis strategies, biological functions to ultrasound-triggered therapeutic applications. Ultimately, the unresolved challenges and clinical-translation potentials of ultrasound nanomedicine and materdicine are discussed and prospected in this evolving field.

Received 3rd December 2022,
Accepted 20th February 2023

DOI: 10.1039/d2tb02640f

rsc.li/materials-b

10th Anniversary Statement

Journal of Material Chemistry B is one of the most significant journals for researchers in the field of ultrasonic medicine to publish research works on ultrasonic nanomaterials. The development of novel ultrasound-responsive nanomaterials has been a hot topic in the field of materials science in recent years and has made new breakthroughs with the development of the *Journal of Material Chemistry B*. I sincerely celebrate the 10th anniversary of the *Journal of Material Chemistry B* and expect to make greater contributions to the development of the journal in the future.

1. Introduction

Nanomedicine has emerged as a simple yet effective approach to address some of the most pressing problems in clinical disease diagnosis and treatment. Particularly, the development of intelligent nanomedicine with exterior physical responsive properties has drawn significant attention due to the accuracy and specificity throughout the theranostic process.[1] Exogenous energy input for theranostic nanomedicine holds great promise when used in conjunction with a variety of triggering sources, including light,[2] ultrasound (US),[3] electric field,[4] magnetic field,[5] *etc.* Even though the non-invasiveness of light-triggered theranostic nanomedicine (photothermal therapy or photodynamic therapy) has attracted considerable interest, the limitation of tissue penetration depth is still the main reason for the improvement of imaging and treatment efficiency.

As a high frequency mechanical wave and typical exogenous energy, US is endowed with the unique characteristics of deep tissue penetration, non-invasiveness, non-ionizing properties, *etc.* It can be used to examine the majority of disorders with systemic organ involvement, such as abdomen, small organs (breast, thyroid, *etc.*), obstetrics and gynecology, musculoskeletal system and blood vessels. As a typical paradigm, contrast-enhanced US imaging as a diagnostic modality that dynamically displays lesions and microvascular components of tissues with microbubbles (MBs) has been widely utilized in clinical practice. In addition to ultrasonic diagnosis, the discipline of ultrasonic medicine has gradually extended to therapy area, including high intensity focused ultrasound (HIFU) and sonodynamic therapy (SDT). A new method called HIFU has been created as an interventional US approach to better fulfill the demands of clinical diagnosis and treatment. Certain nanoagents were created to work in concert with one another to alter the tumor's acoustic microenvironment, which improved the

[a] *Materdicine Lab, School of Life Sciences, Shanghai University, Shanghai 200444, P. R. China. E-mail: chenyuedu@shu.edu.cn*
[b] *Central Laboratory of Shanghai Municipal Hospital of Traditional Chinese Medicine, Shanghai University of Traditional Chinese Medicine, Shanghai 200071, P. R. China. E-mail: changmeiqi@vip.sina.com*
[c] *Shuguang Hospital Affiliated to Shanghai University of Traditional Chinese Medicine, Shanghai, 201203, P. R. China. E-mail: sg_jia_guo@shutcm.edu.cn*
[d] *Department of Shanghai Lung Cancer Center, Shanghai Chest Hospital, School of Medicine, Shanghai Jiao Tong University, Shanghai 200030, P. R. China*
† These authors contributed equally to this work.

effectiveness of HIFU ablation.[6] Furthermore, SDT is a new type of disease treatment method based on low-intensity US with the advantages of non-invasiveness, physical targeting, and low side effects, the kernel of which is to develop safe and efficient US-responsive agents (sonosensitizers) with reactive oxygen species (ROS) production characteristic.

In the past few decades, advancements in nanotechnology and biomaterials have opened up new avenues for ultrasonic diagnosis and treatment.[7] In particular, various nanoscale sonosensitizers, including polymer nanoparticles (NPs), liposomes, carbon-based materials, metal NPs and metal oxides, have been extensively and deeply explored.[8] Nanomaterial-based sonosensitizers have the following benefits above conventional sonosensitizers: (i) a large number of imaging agents or drugs can be loaded into nanomaterials by simple methods due to the existence of enormous space (such as large specific surface area or internal space).[9] (ii) The surfaces of nanomaterials are amenable to physical and chemical modifications, which can significantly improve the target binding capacity and specificity, allowing them to facilitate targeted medication delivery and disease site imaging.[10] (iii) Nanomaterials with appropriate size and surface modification can prolong the blood circulation time and reduce the uptake and clearance by the reticuloendothelial system.[11]

Based on the rapid development of US nanomedicine and materdicine (interdiscipline of materials science and medicine), this review systematically summarizes and discusses the latest progress in US-responsive biomedical applications (Scheme 1). Firstly, the application of sonosensitizers with unique physicochemical properties and specific biological effects in ultrasonic diagnosis and treatment, including SDT, imaging, drug delivery, gene delivery and HIFU, has been discussed in detail. Furthermore, an in-depth insight into the mechanism of US-related therapy and the latest progress of SDT-based synergistic therapy have been provided to excavate the preternatural characteristics of US medicine. Finally, the challenges faced and key issues have been envisioned to further promote the clinical transformation process.

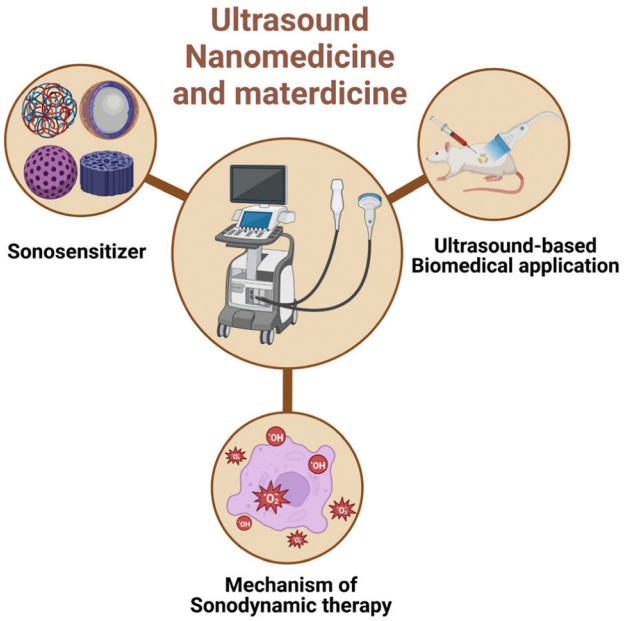

Scheme 1 Schematic illustration of ultrasound nanomedicine and materdicine.

Yu Chen

Prof. Yu Chen received his PhD degree at Shanghai Institute of Ceramics, Chinese Academy of Sciences (SICCAS). He is now a full professor in Shanghai University. His research focuses on materdicine, nanomedicine and nanobiotechnology, which involve the design, fabrication and biomedical applications of mesoporous nanoparticles, two-dimensional nanosheets and 3D-printing bioscaffolds. The focused biomedical applications include drug/gene delivery, catalytic biomaterials, chemoreactive nanomedicine, energetic nanomedicine, theragenerative biomaterials and in situ localized disease therapy. He has published more than 300 scientific papers in nanomedicine field with a total citation of more than 31 000 times (h-index: 94). He is a 2018–2022 Highly Cited Researcher by Clarivate Analytics, Web of Science.

2. Sonosensitizers

2.1 Traditional sonosensitizers

Traditional sonosensitizers are mostly developed based on some small molecule organic compounds with special groups, which are mainly divided into four types: porphyrins, phthalocyanines (Pcs), xanthenes and antitumor drugs.[12–14] Similar to the first-generation photosensitizers, porphyrin-based molecules are the first generation of sonosensitizers commonly used in SDT, including hematoporphyrin (HP), protoporphyrin IX (PPIX), hematoporphyrin monomethyl ether (HMME) and so on.[13] HP is the first reported sonosensitizer, which has been proved to be able to mediate cell damage enhancement *via* singlet oxygen ($^1O_2$) under US activation as early as 1990.[15] PPIX is another important derivative of porphyrin and a classical representative of carboxyl-modified porphyrins.[16] Previous studies showed that PPIX had significant antitumor activities on sarcoma 180 cells under US irradiation.[17] HMME is the second-generation HP-related sensitizer with the characteristics of stable structure, high selectivity and low toxicity.[18] In 2010, Xu *et al.*[19] reported that HMME could synergistically enhance the inhibition effect of UMR-106 cells *via* elevating the intracellular ROS and Ca^{2+} under the US irradiation. Phthalocyanines (Pcs), tetrapyrrole derivatives, are the second generation of photosensitizers. Similar to porphyrins, several studies proved that Pcs can be used as potential sonosensitizers. For instance,

Gabryelak *et al.*[20] found that Pcs combined with US could induce the formation of radicals and subsequently damage the cell membranes. Xanthenes are a special class of oxygen-containing compounds with multiple ring structures, including eosins, fluorescein (FS), and rhodamine, among which Rose Bengal (RB) is the most widely studied sensitizer in anti-tumor therapy.[21] RB, a tetrachloro tetraiodide derivative of FS, has been extensively applied as a photocatalyst.[22] In addition, RB is also employed in the medical field as a sonosensitizer. In 1999, Umemura *et al.*[23] found that the combination of US and RB could induce ultrasonic cavitation and cell damage. Furthermore, US could enhance the lethal effects of anti-cancer and chemotherapeutic agents, such as cisplatin, doxorubicin (DOX), *etc.* Previous study has claimed that DOX could promote the US cavitation, inducing the generation of active oxygen species and hydroxyl radicals ($^{\bullet}$OH), DNA damage and apoptosis.[24]

2.2 Nanomaterial-based sonosensitizers

Due to the low water solubility, poor chemical stability, lack of tumor targeting, and potential skin phototoxicity, the cell retention rate of traditional organic sonosensitizers is limited, thus weakening the therapeutic effect. By comparison, inorganic nanomaterials can be used as excellent substitutes because of the superiorities of multifunctionality, high controllability and low toxicity and side reactions.

2.2.1 Titanium dioxide nanomaterials. Titanium dioxide (TiO_2), as a typical inorganic semiconductor, is a natural oxide of the element titanium with low toxicity.[25] As a typical photosensitizer, TiO_2 nanomaterials could cause the overproduction of ROS and suppress the tumor growth through facilitating the separation rate of electron–hole pairs under ultraviolet (UV) light irradiation. However, the therapeutic effect on the deep tumors falls short of expectations due to the low penetrability of UV light. To overcome this limitation, a lot of researchers have recently started to explore the function of TiO_2 as a sonosensitizer in SDT. Tachibana *et al.*[26] reported that the combination of TiO_2 and US showed significant inhibition of melanoma tumor growth *in vitro* and *in vivo*. However, it is challenging for bare TiO_2 NPs to collect in large quantities within tumor tissue and stabilize in the physiological environment. Various modified TiO_2 nanomaterials including polyethylene glycol (PEG)-modified TiO_{1+x} nanorods and W-doped TiO_2 (W-TiO_2) nanorods were rationally designed and synthesized.[27,28] As a typical paradigm, Shimizu *et al.*[29] anchored avidin to the surface of TiO_2 NPs, which selectively recognized HepG2 cells and exhibited excellent uptake performance for targeted and efficient SDT.

2.2.2 Noble metal nanomaterials. The ingenious combination of noble metal materials (Au, Ag and Pt) and nanomaterials can be used to increase the effectiveness of SDT through blocking of the electron–hole recombination and enhancing the ROS generation. Yeung *et al.*[30] fabricated Au@Cu_2O hybrid nanocubes by integrating Au NPs onto the surface of Cu_2O (Fig. 1(A)). The electrons from Cu_2O could be stimulated at the junction and transferred to Au under US irradiation to extend the electron–hole separation rate and limit the reflux of US-triggered electrons, which could be attributed to the formation of a Schottky contact (Fig. 1(B)). Owing to the enhanced electron–hole separation efficiency, the Au@Cu_2O hybrid nanocubes could create the excessive ROS to reinforce the bactericidal capacity in the presence of US (Fig. 1(C) and (D)). Furthermore, the sonodynamic activity of the Au@Cu_2O hybrid nanocubes could be regulated through changing the ratio of Au on the Cu_2O nanocube surface. In addition, Jae Hyung *et al.*[31] reported that hydrophilized Au–TiO_2 nanocomposites improved the SDT efficiency by generating a large amount of ROS, completely leading to the inhibition of tumor growth upon exposure to US. Li *et al.*[32] developed the α-Fe_2O_3@Pt heterostructure NPs, which promoted ROS induction due to the valid separation of US-excited electrons and holes. In particular, α-Fe_2O_3@Pt NPs showed the intrinsic catalase-like activity, enabling the catalysis of hydrogen peroxide (H_2O_2) and the self-supply of O_2 to relieve the tumor hypoxia.

2.2.3 Transition metal oxide nanomaterials. With the exception of titanium-based nanomaterials, several transition metal (iron and manganese) oxides can also be applied for US-related therapies. For example, Liu *et al.*[33] synthesized a new-type sonosensitizer based on ultrasmall anoxic bimetallic oxide $MnWO_X$ nanoparticles for multimodal imaging-guided enhanced SDT. The $MnWO_X$ nanoparticles modified by PEG exhibited high physiological stability and biocompatibility. Since the anoxic structure of $MnWO_X$ can be used as an electron trap site to inhibit *in situ* electron hole recombination, the generation of $^1O_2$ and $^{\bullet}$OH can be efficiently triggered by the as-prepared $MnWO_X$-PEG nanoparticles under US irradiation. In addition, $MnWO_X$-PEG had excellent capacity of glutathione consumption, which further enhanced the SDT-induced tumor killing. Computed tomography and magnetic resonance imaging (MRI) showed that $MnWO_X$-PEG could effectively destroy tumor in mice under US stimulation and was metabolized by mice after completing the treatment without long-term toxicity.

In addition, Fe-doped TiO_2 nanodots (Fe–TiO_2 NDs) with ultrasmall size as a kind of nanoplatform have been developed for enhanced SDT and feature prominent biocompatibility after PEGylation.[34] By narrowing the band gap, the acquired Fe–TiO_2-PEG NDs were proved to exhibit superior sonodynamic activity than bare TiO_2 NDs. Moreover, Fe–TiO_2-PEG NDs could generate a large number of ROS through a Fe-dependent Fenton reaction, ultimately enabling the apoptosis of tumor cells through the combination of SDT and chemodynamic therapy (CDT) (Fig. 2(A)).

2.2.4 Carbon-based nanomaterials. Carbon-based nanomaterials have attracted extensive research interest for years owing to their unique mechanical, electrical, and optical properties, such as zero-dimensional fullerene, one-dimensional carbon nanotubes, two-dimensional (2D) graphene, and graphene oxide.[35,36] Lin *et al.*[37] synthesized a carbon-doped TiO_2 sonosensitizer through anchoring carbon into the anatase structure of TiO_2 to generate ROS for cancer treatment under the activation of low-intensity US. The addition of carbon could accelerate electron hole transfer rate through decreasing the bandgap (Fig. 2(B)). Chen *et al.*[38] reported 2D nanocomposites

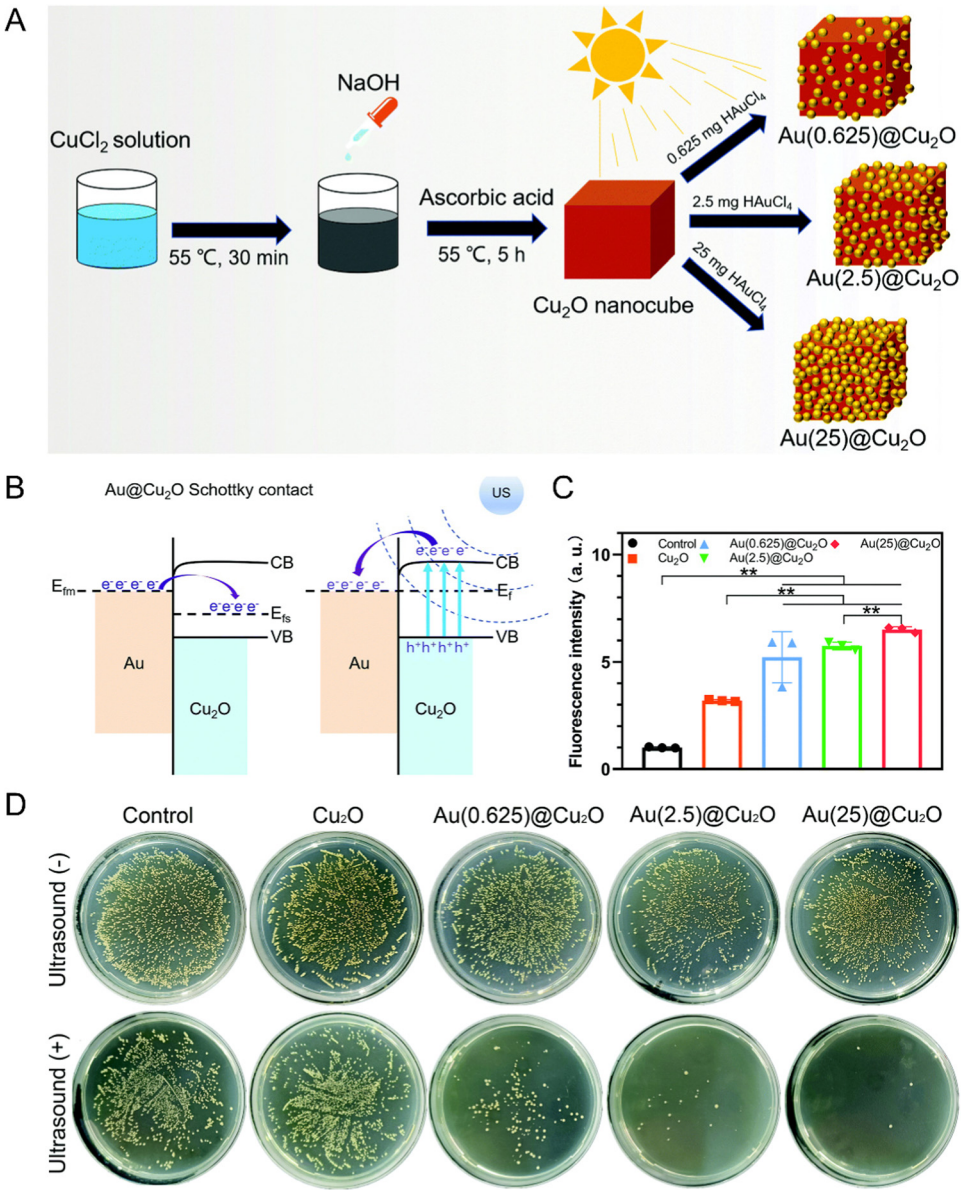

Fig. 1 (A) Schematic illustration of the synthetic process of Au@Cu_2O hybrid nanocubes. (B) Schematic diagram of a Schottky contact between Au and Cu_2O. (C) ROS generation abilities of different samples detected by the fluorescence intensity of DCF. n = 3 independent experiments per group; *$P < 0.05$ and **$P < 0.01$. (D) Spread plates of different samples with or without US stimulation. Reproduced with permission.[30] Copyright 2021, Royal Society of Chemistry.

(MnO_x/TiO_2-GR) composed of 2D reduced GO (GR) nanosheets with TiO_2 for enhancing the SDT efficiency to combat cancer. The presence of GR nanosheets effectively facilitated the separation of e^- and h^+ based on their high electro-conductivity and larger surface area to generate more ROS. In addition, the superior photothermal-conversion properties of GR could synergically improve SDT efficiency by photothermal effects (Fig. 3). Shen *et al.*[39] investigated the killing effect of platinum crosslinked carbon dot@TiO_{2-x} p–n junctions (Pt/N-CD@TiO_{2-x}) on osteosarcoma. The results exhibited that malignant osteosarcoma cells were fully exterminated without recurrence *via* intravenous injection of a small quantity of Pt/N-CD@TiO_{2-x} combined with US irradiation.

2.2.5 MOF-based sonosensitizers. Metal–organic frameworks (MOFs) represent a class of highly ordered crystalline porous coordination polymers (PCPs), which are formed by self-assembly of metal (such as transition metals and lanthanide metals) ions or clusters and organic ligands (such as carboxylates, phosphonates, imidazole salts and phenolic salts) through coordination bonds. Compared with other solid porous materials, MOFs have the outstanding advantages that the pore size and function of the obtained materials can be designed and controlled by selecting different metal ions, organic ligands, functional groups and activation methods.[40] Due to the fact that nearly all metals and various organic compounds can be used for the preparation of MOFs, a variety

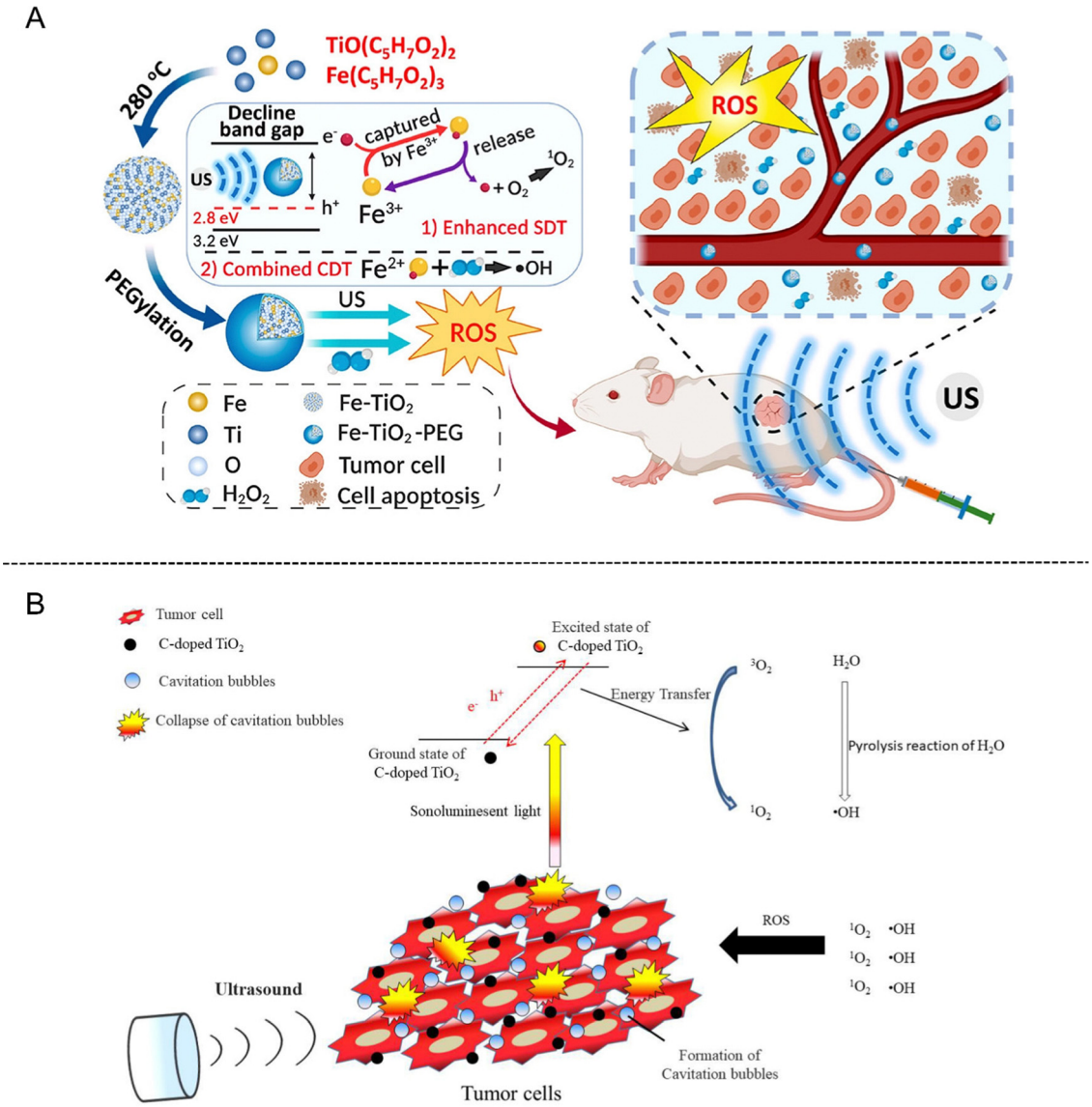

Fig. 2 (A) Schematic illustration of ultrasmall Fe–TiO_2 NDs for dual-modal imaging-guided SDT/CDT combined therapy. Reproduced with permission.[34] Copyright 2020, American Chemical Society. (B) Schematic illustration of C-doped TiO_2 for SDT in cancer therapy. Reproduced with permission.[37] Copyright 2020, Multidisciplinary Digital Publishing Institute.

of MOF materials with unique structures and properties have emerged, such as UiO-66,[41] HKUST-1,[42] ZIF-8[43] and ZIF-67.[44]

Unique properties of MOFs and their derivatives, including their highly organized structure, high surface area, and huge pore volume, allow functional molecules to bind to their surfaces or pore channels. Based on the above advantages, MOF-based nanomaterials as the carrier of sonosensitizers have been applied to improve the therapeutic effect of SDT. For example, Huang *et al.*[45] embedded the oxygen-independent sonosensitizer (AIPH) into the oxygen-dependent sonosensitizer (Zr-MOF), thus developing a double-sonosensitizer nanoplatform (Zr-MOF@AIPH). Under the stimulation of US, the Zr-MOF can react with oxygen to generate $^1O_2$, while AIPH can decompose to generate alkyl free radicals and enhance the therapeutic effect of SDT under normal oxygen environment, ensuring its killing ability against hypoxic tumor. In addition, nitrogen (N_2) generated by AIPH decomposition can further promote tumor infiltration of Zr-MOF@AIPH through ultrasonic cavitation effect. Therefore, the double-sonosensitizer nanoplatform can be used as an effective strategy for the treatment of hypoxic tumors.

Traditional organic sonosensitizers such as porphyrins and their derivatives have no significant sonodynamic effect owing to the lack of accumulation at the tumor sites. Although the introduction of auxiliary nanoparticles in the sonosensitizer system has improved the sensitivity of sonodynamic therapy to some extent, the clinical application of this composite system is limited by the poor stability, complex process and high cost.[13] Therefore, it is extremely challenging to develop a new type of sonosensitizer to solve the above problems. Recently, the

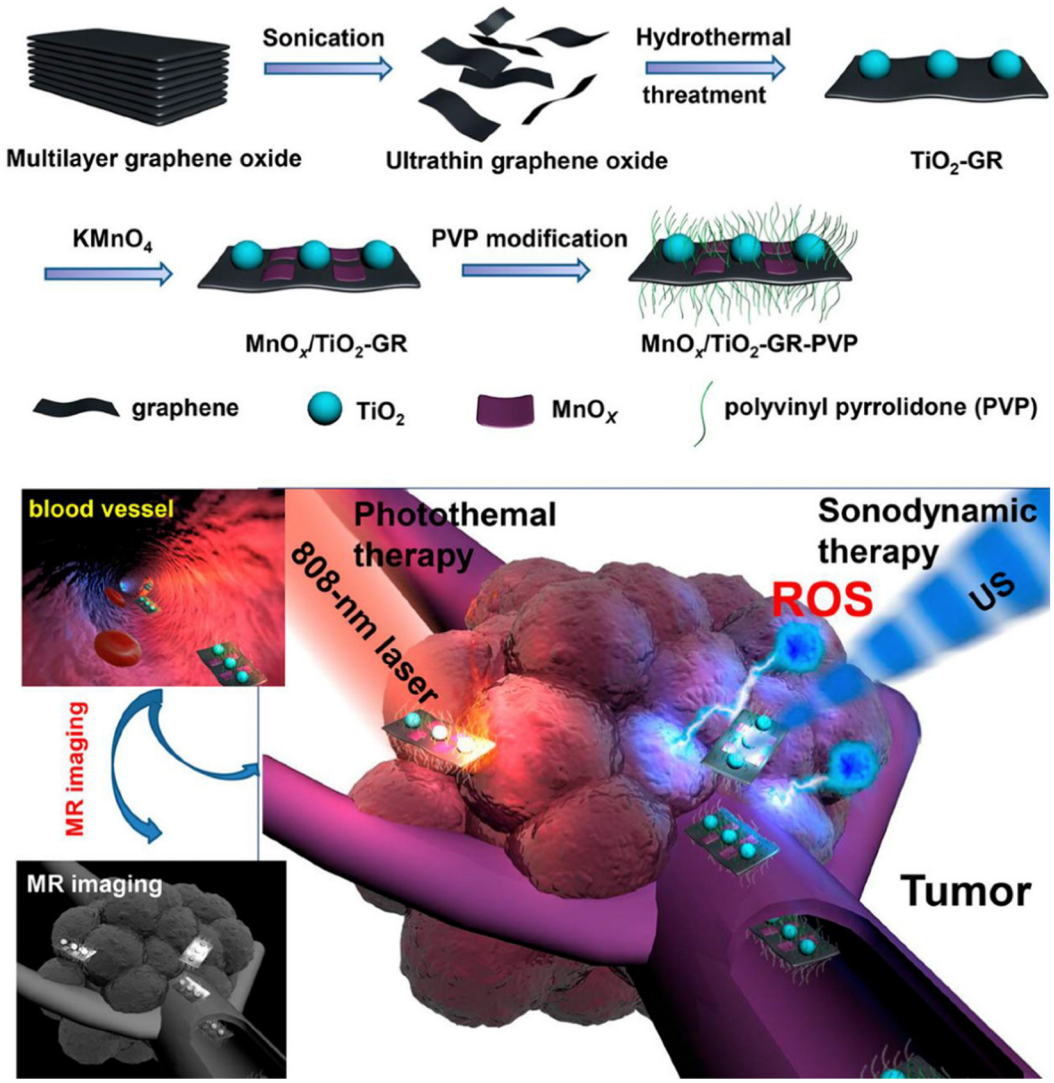

Fig. 3 Schematic illustration of the synthetic procedure of MnO_x/TiO_2-GR-PVP and MR imaging-guided synergistic SDT/PTT against cancer. Reproduced with permission.[38] Copyright 2017, American Chemical Society.

sonodynamic characteristics of porphyrin-based MOF materials have also been developed. For instance, Liu *et al.*[46] synthesized mesoporous carbon spheres with porphyrin-like structure (designated as PMCS) by high-temperature calcination using zeolite imidazole based framework material (ZIF-8) as a template, and the sonodynamic sensitization of PMCS has been explored. The density functional theory (DFT) calculation results unveiled that the high production efficiency of ROS in PMCS is highly related to the porphyrin-like structure. In addition, the high specific surface area and multi-channel structure enable PMCS to carry a large number of gas cores, enhancing the cavitation effect of US. The *in vivo* results proved that PMCS has preeminent biocompatibility and excellent tumor inhibition efficiency (Fig. 4(A)). Moreover, Lu *et al.*[47] designed a multifunctional manganese porphyrin-based metal–organic framework (Mn-MOF) to stimulate the generation of ROS and ferroptosis upon US exposure. Considering that manganese porphyrins possess catalase-like activity that can mediate single electron reversible transfer, Mn-MOF could continuously decompose H_2O_2 to O_2 at the hypoxic tumor site, reducing the extent of hypoxia and accelerating the ROS production (Fig. 4(B)).

3. US-based biomedical application

3.1 US imaging

US imaging, as a conventional detection method in clinic, has been extensively used in detecting the size, shape, internal structure, blood vessel distribution and activity of various organs for disease screening, location and qualitative diagnosis.[48] The US imaging of internal organs could be obtained by receiving and processing the ultrasonic echo signals by scanning the human body with ultrasonic waves. However, the general US imaging is insufficient to accurately diagnose disorders associated with poor blood vessel distribution and

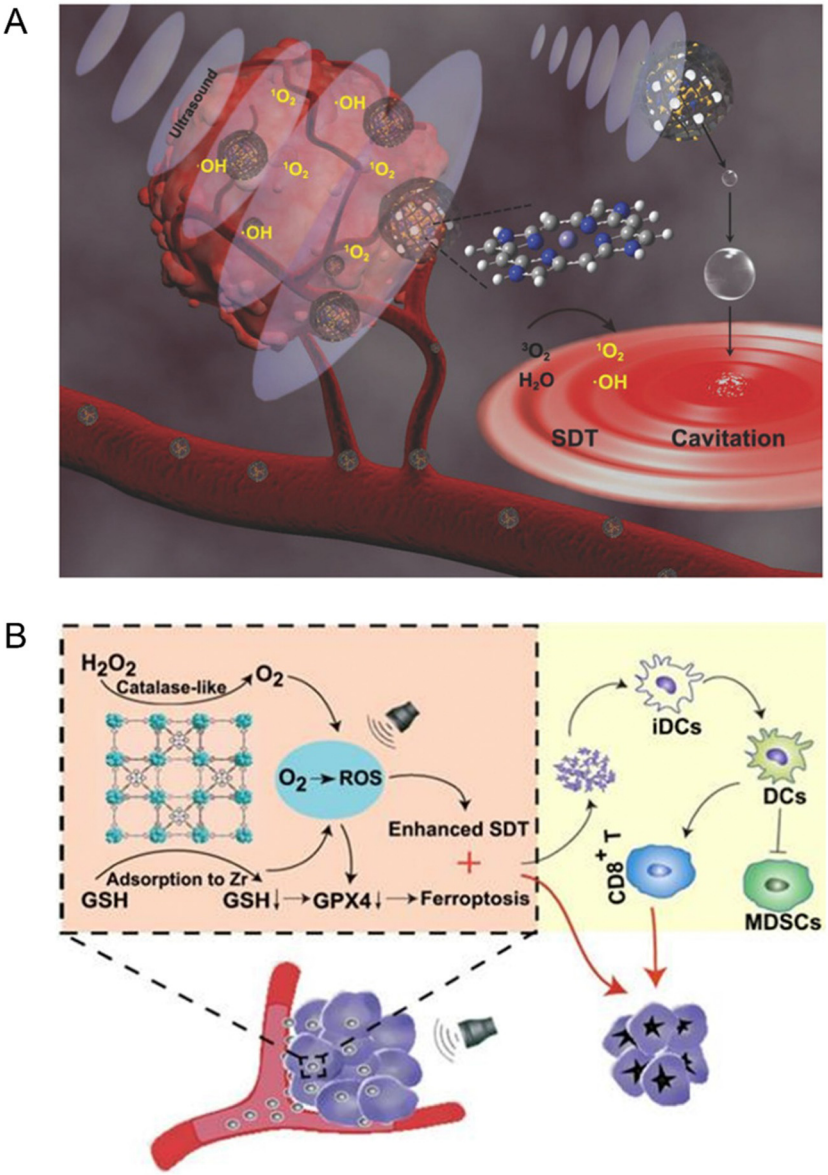

Fig. 4 (A) Schematic illustration of the sonosensitization process of PMCS for cancer therapy. Reproduced with permission.[46] Copyright 2018, Wiley-VCH. (B) Schematic illustration of Mn-MOF for enhanced SDT and ferroptosis in cancer therapy. Reproduced with permission.[47] Copyright 2021, Ivyspring International.

blood flow deceleration. Based on this background, the contrast agents have been developed and utilized in US imaging to significantly improve the resolution, sensitivity and specificity of ultrasonic diagnosis due to the characteristics of tissue echo enhancement.[49] These agents are generally classified into two types, MB contrast agents and NP contrast agents.

MBs (1–10 μm in average size) are a type of small hollow spheres composed of outer membranes and wrapped gas, which are normally stabilized by coating albumin, phospholipid and polymer layers,[50,51] which can not only inhibit the filled-gas from escaping, but also prevent the mutual fusion between MBs. The gas encapsulated by MBs is composed of a macromolecular gas or inert gas (such as a fluorocarbon gas) with preferable acoustic backscattering and reflection effects, which can be safely discharged from the lungs.[52] Under ultrasonic excitation, such a gas can magnify the echo for enhancing the tissue imaging. However, the micron scale MBs cannot penetrate through the vascular endothelial gap of tumor due to size limitation, resulting in a short tumor retention time. To circumvent these shortcomings, NP-based contrast agents with the penetrating ability through vascular endothelium cells have been rationally developed for the extravascular imaging, such as perfluorocarbon (PFC)-based NPs and silica NPs.

PFC NPs have a liquid core with a diameter of about 200–250 nanometers, which are encapsulated by a phospholipid monolayer and could be emulsified by microfluidic technology at 20 000 psi.[53] PFC emulsions have been approved as artificial blood substitutes for oxygen delivery due to their high oxygen

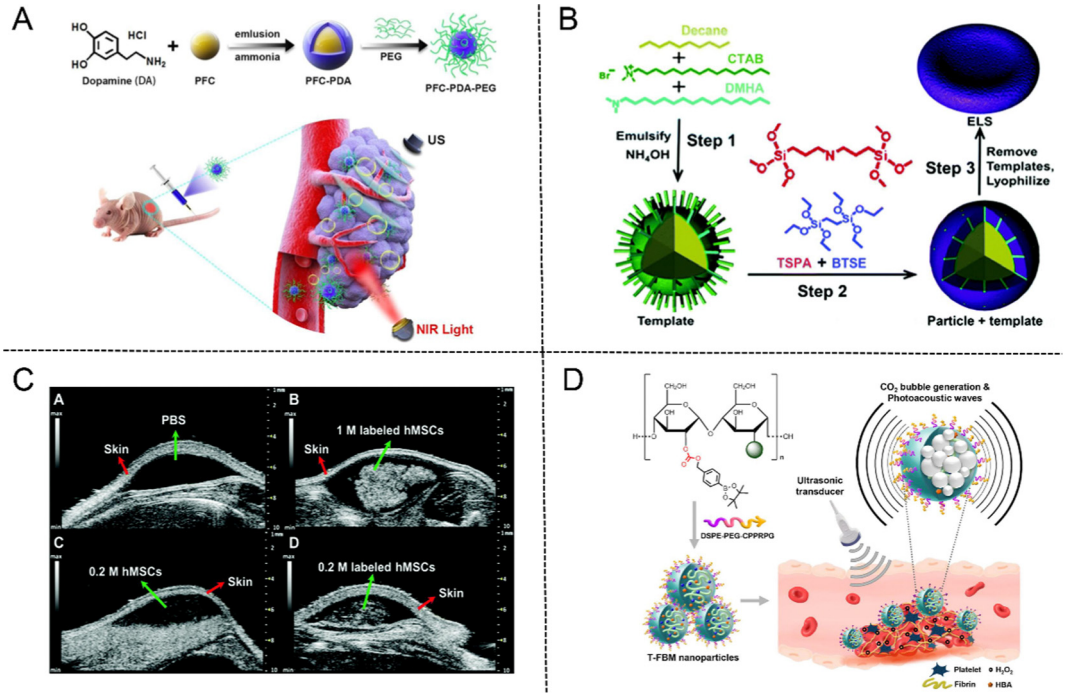

Fig. 5 (A) Schematic illustration of PFC-PDA-PEG nanoparticles for US imaging and PTT. Reproduced with permission.[56] Copyright 2020, American Chemical Society. (B) The fabrication process of ELS nanoparticles. (C) *In vivo* US imaging of unlabeled and ELS-labeled hMSCs. Reproduced with permission.[57] Copyright 2017, Royal Society of Chemistry. (D) Schematic illustration of T-FBM nanoparticles as a H_2O_2-triggered photoacoustic signal amplifier. Reproduced with permission.[60] Copyright 2018, American Chemical Society.

carrying capacity, biochemical inertia and excellent biocompatibility. In addition, PFC emulsions are utilized as significant components of US contrast agents for their comparatively low acoustic impedance to soft tissues.[54] Furthermore, PFC NPs in combination with droplet vaporization are also a growing issue and subject of research. PFC nanodroplets can undergo liquid–gas phase transition to vaporize into gaseous MBs *in situ* for US imaging when they are subjected to acoustic activation or heat.[55] Cao *et al.*[56] developed polydopamine (PDA)-based PFC NPs (designated as PFC-PDA-PEG) by encapsulating PFC nanodroplets into PDA modified by PEG-NH_2. *In vitro* and *in vivo* experiments demonstrated that PFC-PDA-PEG possesses high photothermal conversion efficiency which can generate a large amount of heat to eliminate tumor cells under exposure to near-infrared (NIR) laser irradiation, meanwhile, superheated PFC droplets will absorb heat and evaporate from liquid into gas phase for US imaging (Fig. 5(A)).

In recent years, hollow silica NPs as the typical contrast agents have attracted much attention due to their echo generation characteristics for US imaging. Jokerst *et al.*[57] fabricated exosome-like silica (ELS) NPs for stem cell imaging with an emulsion soft-template composed of hexadecyltrimethylammonium bromide (CTAB), dimethylhexadecylamine (DMHA), and decane (Fig. 5(B)). The *in vitro* echogenicity of the ELS NPs was then compared to those of three conventional silica NPs, including the Stöber silica nanospheres (SSN), the MCM-41 mesoporous silica nanospheres (MSN), and the mesocellular foam silica NPs (MCF). The results showed that ELS displayed the strongest echogenicity among four NPs after being scanned in an agarose phantom at 40 MHz. ELS could produce the same US contrast at a lower dose due to the higher echogenicity, thus enhancing its biocompatibility. In addition, *in vivo* US images of ELS-labeled human mesenchymal stem cells (hMSCs) exhibited remarkable echogenicity compared to unlabeled cells due to the enhanced cellular uptake efficiency and intrinsic increased echogenicity of ELS NPs (Fig. 5(C)).

Moreover, US imaging is frequently utilized in conjunction with photoacoustic (PA) imaging to address the issue of weak specificity and spatial resolution and enhance the accuracy of diagnosis. As a non-invasive medical imaging modality based on the PA effect, PA imaging exhibits the advantages of high contrast of optical imaging and deep penetration of ultrasonic imaging by converting absorbed light energy into acoustic energy. The PA effect was first reported by Bell in 1880 and began to be applied in the field of material testing in the 1970s.[58] With the further development of ultrasonic detection technology and data acquisition system and computing power, PA technology was gradually applied in the biomedical field.[59] For example, Lee *et al.*[60] prepared H_2O_2-triggered thrombus-targeted therapeutic (T-FBM) NPs *via* conjugating borylbenzyl carbonate and fluorescent IR780 to maltodextrin. Both US and PA signals were enhanced through production of CO_2 bubbles stimulated by H_2O_2. Meanwhile, T-FBM NPs exerted significant therapeutic effects on inhibiting thrombus formation (Fig. 5(D)).

3.2 US-triggered drug release

Many pharmaceuticals used to treat conditions including cancer, eye illnesses, and brain diseases induce negative side

effects. The drug dose must be closely controlled under certain circumstances. Drug delivery systems (DDS), such as polymeric NPs and liposomes, have been extensively investigated in an effort to overcome the drawbacks and limitations of conventional medications. Previous research reported that US has been applied to deliver drugs to various tissues for more accurate therapy and enhanced SDT efficiency.[61] At present, MBs are the most researched and widely used US-responsive drug delivery carriers,[62] which can be concentrated into tumor tissues under the combined action of enhanced permeability and retention (EPR) effect and active targeting. The medicine in MB can be released into the tissue by creating a shock wave, microflow and microjet and can be monitored by US imaging when transient cavitation occurs.[63] Zheng *et al.*[64] reported a PTX-liposome-MB complex (PLMC) for drug delivery in breast cancer treatment. Compared with the bare PTX-liposome group, PLMC showed 3.5-fold higher PTX distribution in tumors.

However, the micrometer-scaled MBs find it difficult to penetrate the vascular endothelial barrier and accumulate in the surrounding tumor tissues.[65] Hence, the appropriate nano-sized sonosensitizers were exploited to deliver the drugs with the specific dose in a controllable manner and alleviate the systemic toxic effects. Shuai *et al.*[66] fabricated size-adjustable PFP/PFB/DOX-PPEHD nanosystems for drug delivery against cancer. PFP/PFB/DOX-PPEHD nanosystems at the tumor site could be activated under the irradiation of low-frequency US (LFUS), leading to the rapid release of DOX and the efficient uptake of tumor cells. In addition, such a LFUS-triggered nanosystem delivery allowed the medicine to penetrate the tumor through the EPR effect and maintain a nanoscale suited for long-term blood circulation, solving the delivery bottleneck of nano-carriers (Fig. 6). Yang *et al.*[67] reported a US-activated asparagine–glycine–arginine (NGR)-modified liposomal nano-carrier (NGR/UT-L) combined with a lipophilic sonosensitizer, chlorin e6 (Ce6) ester and DOX. Owing to the targeting characteristic of NGR, NGR/UT-L could accumulate in the tumor sites of HT-1080 tumor-bearing mice. In addition, the blood concentration-time curve exhibited that DOX of NGR/UT-L displayed a 3.9-fold level of blood drug concentration than free DOX. The breakdown of the lipid bilayer could mediate the release of wrapped DOX, as induced by US irradiation. The above experimental results demonstrated that NGR/UT-L was a smart drug delivery system *via* the combination of tumor-targeted

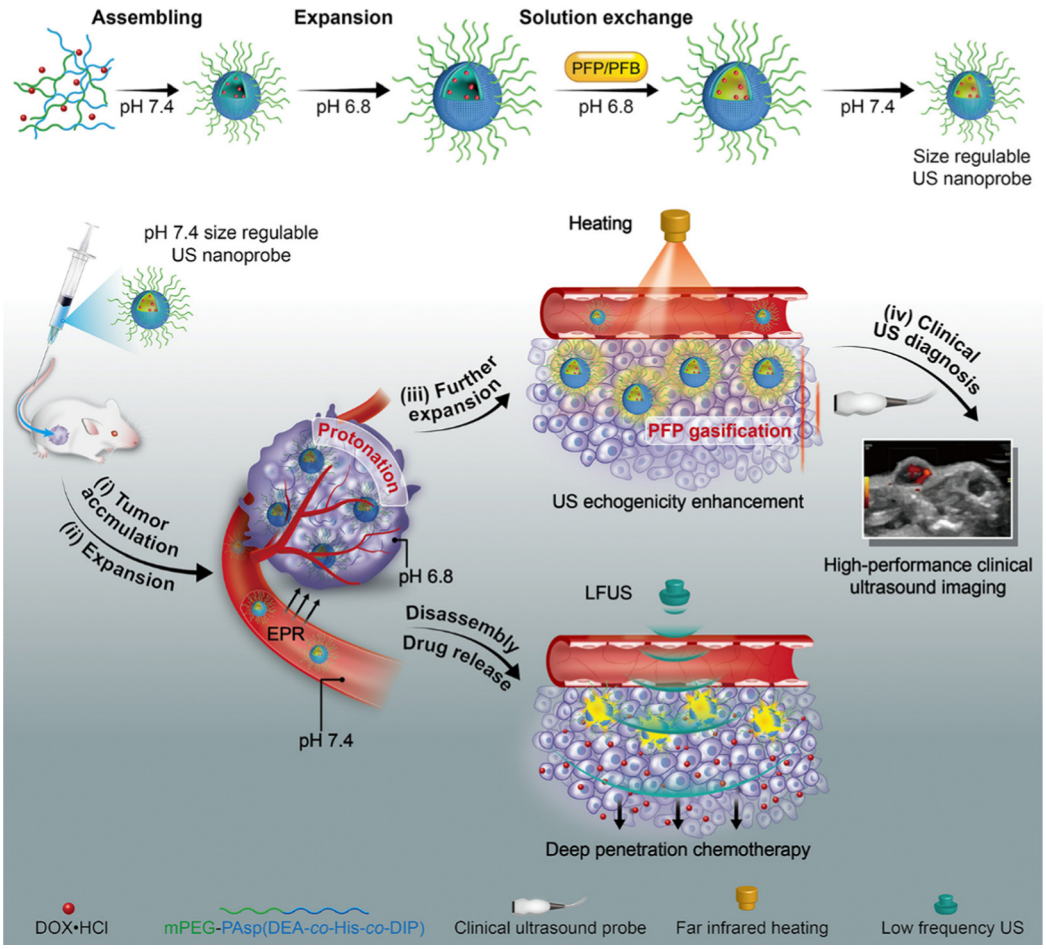

Fig. 6 Schematic illustration of PFP/PFB/DOX-PPEHD nanosystems for US imaging and drug delivery against cancer. Reproduced with permission.[66] Copyright 2018, American Chemical Society.

property and controlled release characteristic. Kotopoulis *et al.*[68] performed the first clinical study on the combination of chemotherapy and MBs for pancreatic cancer over 31.5 minutes. After several treatment cycles, the tumor size of two out of five patients temporally or permanently decreased by 70–80% and even resumed to original size eventually, while the tumor growth of the remaining patients was also inhibited to varying degrees.

3.3 US-triggered gene delivery

The US-mediated gene delivery including a series of nucleic acids, such as plasmid DNA (pDNA), microRNA (miR), messenger RNA (mRNA), short hairpin RNA (shRNA) and small interfering RNA (siRNA), is an efficient therapeutic modality for various diseases to improve off-target delivery issue and enhance the gene transfection.[69] The important premise of effective gene therapy lies in the selection of vectors and targeted gene delivery. Compared with traditional vectors (viruses, plasmids, *etc.*), MBs are a new-type, safe, stable and potential gene delivery vector.[70] However, with the in-depth study of MBs, many researchers found that it was difficult for MBs to enter the surrounding tissues through the vascular wall due to their large particle size, which greatly reduced their bearing capacity.[71] Therefore, reducing the particle size of MBs as much as possible became a research hotspot. At present, MBs used for contrast-enhanced US generally have a diameter of 1–10 micrometers, which is approximately equal to the size of a red blood cell, thus limiting their exudation from blood vessels to tissues.[72] In recent years, nanotechnology can be used to prepare MBs with smaller particle size, namely nanobubbles (NBs), to make their particle size reach the nanometer level, providing more possibilities for MBs to be utilized for gene delivery. In 2009, Kodama *et al.*[73] implied that NBs could modulate the gene transfer to targeted skeletal muscle in nude mice with the sonication treatment. In addition, this is the first paradigm about the isotopic imaging (PET or SPECT) for visualization of NB-induced gene delivery, which established a new method to test nontraditional gene delivery in patients with hereditary diseases including muscular atrophy and vascular disorders. Wang *et al.*[74] synthesized isocitrate dehydrogenase 1 (IDH1)-siRNA-loaded NBs by utilizing octafluoropropane (C_3F_8) gas and phospholipids as the core and shells, respectively. The results signified that the NBs had a remarkable effect on the expression of IDH1 and inhibited glioma tumor growth *in vitro* and *in vivo*. Lu *et al.*[75] evaluated the effects of micelles encapsulated with three different pluronics (F127, L61 and P85) on gene delivery in 3T3-MDEI, C2C12, and CHO cell lines. The results revealed that pluronics combined with US synergistically enhanced the gene transfection efficiency in a dose-dependent manner. However, the delivery efficiency obviously decreased when treated with US alone.

3.4 High intensity focused US

High intensity focused US (HIFU) is a brand-new and attractive therapeutic modality in the treatment of various solid cancers and other diseases. The technique known as ''HIFU'' involves the high-intensity ultrasound produced by a piezoelectric transducer with alternating voltage, which can be focused into a small focal spot through a certain focusing method to ablate the targeted tissue.[76] HIFU mainly functions through two mechanisms: thermal effects and mechanical effects.[77] As is known to all, US is a kind of mechanical wave that oscillates periodically and has strong tissue penetration ability.[78] When HIFU penetrates the lesion sites, the diseased tissue will absorb mechanical energy and release heat, namely the thermal effect. Due to its thermal effect, the heat generated by HIFU can rapidly increase the temperature of target tissue to more than 60 °C. Target cells will experience irreversible coagulative heat necrosis if the temperature persists for longer than one second. As ultrasonic waves tend to focus on a small-area focal point with a diameter of 1 mm, this minimizes the potential damage to tissues outside the focal area. In addition to thermal effect, mechanical effect is the other typical feature.[79] Tissue cells vibrated frequently under the action of HIFU. When it exceeds the elastic limit, tissue would be damaged by causing the flow of cytoplasm, protein deformation, altered cell function, breakdown of DNA macromolecules, and protein denaturation.[80] In addition, the mechanical effects of HIFU are only relevant to high-intensity acoustic pulses, which are based on microstreaming, radiation force and cavitation.[81] Lee *et al.* conducted a retrospective study to evaluate the HIFU ablation effects on the non-advanced hepatocellular carcinoma (HCC) patients, who were divided into a HIFU + trans-arterial chemoembolization (TACE) group and a TACE group. The results suggested that TACE combined with HIFU significantly improved the median survival time and cumulative survival rate of the tumor patients compared to TACE monotherapy.[82] However, HIFU has many inevitable application defects in deep tissues, such as acoustic energy with exponential decay, superfluous heating and increased damage probability of tissue. Based on these critical issues, MBs as potential HIFU synergists have been applied to overcome these troublesome challenges. Some related researches indicate that the mechanism of MBs-enhanced HIFU therapeutic efficacy might be attributed to the acoustic cavitation of HIFU.[83] Choi *et al.* testified that the addition of MBs synergistically enhanced chemotherapy effects of gemcitabine combined with HIFU in the pancreatic cancer xenograft models.[84] Nevertheless, MBs still suffer from some non-negligible deficiencies as the HIFU synergistic agents, including large particle sizes, easy-cracking, short half-life and low stability.

Very recently, a variety of NPs have displayed excellent performance in diagnostic imaging and tumor treatment combined with HIFU for their smaller dimension and superior stability. Dayton *et al.*[85] developed a phase-changeable NP with enhanced HIFU ablation efficiency by transforming into a MB only when it is exposed to acoustic pressure. The synergistic enhancing effects on HIFU ablation were investigated by comparing the ablation volume generated in rats' livers during sonication. The results displayed that NPs and MBs were all able to enhance the HIFU-mediated liver ablation efficiency. NPs did not cause skin burns or undesirable off-target thermal ablation, demonstrating their preferred therapeutic biosafety *in vivo*.

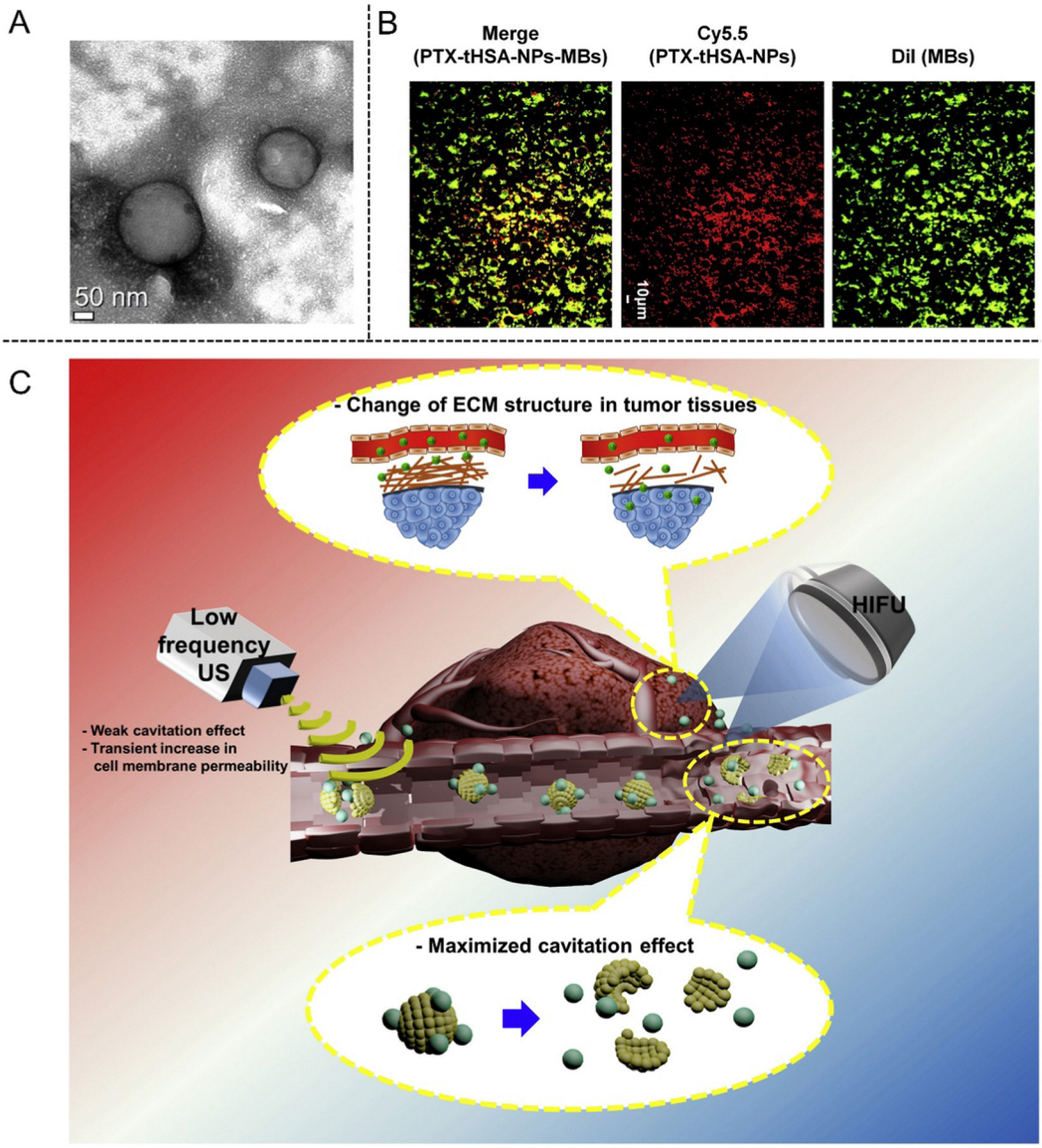

Fig. 7 (A) TEM image of PTX-tHSA-NPs. (B) Fluorescence microscopy images of MBs (green), PTX-tHSA-NPs (red), and PTX-tHSA-NPs-MBs (yellow) for identifying conjugation. (C) Schematic illustration of the delivery of PTX-tHSA-NPs-MBs under HIFU radiation. Reproduced with permission.[86] Copyright 2017, Elesvier.

Except for the ultrasonic ablation, HIFU has also been developed as supplementary means for drug delivery owing to its adjustable membrane permeability. In 2017, Kim *et al.*[86] constructed a HIFU-enhanced drug delivery system composing of paclitaxel-loaded thiolated human serum albumin NPs and MBs (PTX-tHSA-NPs-MBs), which was demonstrated to enhance anti-cancer efficacy in A549 tumor-bearing mice with HIFU exposure. In addition, circulating PTX-tHSA-NPs-MBs in the blood stream around the tumor site could be triggered by HIFU exposure, which resulted in the release of PTX-tHSA-NPs and their increased accumulation inside the tumor (Fig. 7(A)–(C)).

With the rapid development of precision medicine and nanobiotechnology, traditional imaging-guided HIFU ablation is incapable of satisfying the clinical demands. However, it is exhilarating that the advent of multifunctional NPs can make up for such defects as HIFU synergistic agents in order to achieve the enhanced therapeutic efficiency. Recently, Li *et al.*[87] fabricated a biocompatible multifunctional nanosystem (designated as Fe_3O_4-PFH/PLGA) composing of the super-paramagnetic Fe_3O_4-integrated PLGA capsules and PFH (perfluorohexane). Super-paramagnetic Fe_3O_4/PLGA nanocapsules can sensitize a tumor to the effects of hyperthermia. Furthermore, hydrophobic PFH loaded into the core of Fe_3O_4/PLGA nanocapsules could be vaporized by the thermal effect of HIFU because of its desirable boiling point of 56 °C. Such a phase-changing and bubble-generation procedure was successfully demonstrated to improve the performances of HIFU treatment in rabbit liver tumor model. In particular, the Fe_3O_4-PFH/PLGA NPs had a tri-modality imaging function, which can be used for imaging-guided HIFU ablation.

3.5 SDT-based therapy

SDT is a modality of non-invasive disease treatment, which can be used in the treatment of cancer, bacterial infections, and vascular diseases.[88] Compared with traditional treatment methods, SDT is able to penetrate deep tissues and induces less damage to normal cells and tissues, providing a new choice for clinical treatment. Similar to photodynamic therapy (PDT), the underlying mechanism of SDT originates from the interaction between US and sonosensitizer. Sonosensitizers that are concentrated in disease locations are activated to produce harmful ROS against pathogenic cells when exposed to low-intensity US (0.5–4.0 W cm^{-2}) radiation.[89] Despite the fact that SDT has demonstrated considerable promise in the cancer treatment, the heterogeneity, complexity and flexibility of the tumor microenvironment make it highly challenging to achieve the desirable therapeutic impact with monotherapy. In this section, several SDT-based therapeutic strategies are comprehensively summarized and discussed.

3.5.1 SDT combined with chemotherapy. Chemotherapy is one of the most effective therapeutic modalities in clinic, which uses chemically synthesized drugs to kill tumor cells or inhibit tumor growth. However, chemotherapy medications frequently induce undesirable and severe side effects on a significant number of normal cells and tissues due to their poor targeting abilities, which prevents them from effectively killing tumor cells and suppressing the immune system. In addition, chemotherapy drugs can induce the dysfunction of bone marrow hematopoietic stem cells and the developed tumor chemoresistance. Thus, a focus of the research on tumor treatment is the alternative therapeutic modalities to decrease chemoresistance and improve sensitivity of malignancies to chemotherapeutic medicines. Recent studies have demonstrated that employing low-intensity US can improve the chemotherapeutic effect and selectively enhance the tumor cell uptake of chemotherapeutic drugs, thereby alleviating the drug resistance induced by drug efflux.[90] Therefore, the rational combination of SDT and chemotherapy is an efficient strategy for cancer treatment by achieving a synergistic therapeutic effect and outcome.

SDT has shown the triggered antitumor immunity capability by eliciting immunogenic cell death (ICD).[91] However, SDT can lead to the aggravation of hypoxia and exposure of platelet (PLT)-associated danger-associated molecular patterns (DAMPs) owing to the dependence of oxygen consumption, which would seriously compromise the therapeutic efficacy and contribute to tumor angiogenesis and metastasis. To solve this critical issue, Wang *et al.*[92] prepared a biomimetic decoy (designated as Lipo-Ce6/TPZ@MH) by loading sonosensitizer chlorin e6 (Ce6) and hypoxia-activated tirapazamine (TPZ) in the red blood cell-PLT hybrid membrane (MH)-camouflaged pH-sensitive liposome, which could more easily accumulate into tumor sites by inducing immune escape and specifically focus on the targeted area through biomimetic surface modification. ROS generation and TPZ activation have demonstrated a positive synergistic therapeutic effect under US irradiation. Simultaneously, the decoy retained the PLT-binding function but did not involve the PLT-mediated metastasis, thereby repressing the DAMP-triggered tumor metastasis. Furthermore, ICD-induced antitumor immunity eradicated the residual tumor tissues following synergistic treatment of SDT and chemotherapy.

Autophagy refers to a highly conserved process in which damaged proteins and organelles are self-degraded by lysosomes in cells, which plays a vital role in maintaining cellular homoeostasis by regulating various physiological and pathological processes.[93] Owing to the specific interrelation of tumor and autophagy, autophagy regulation-related tumor therapy has become an important strategy in clinical disease treatment. The ROS production, such as $^1O_2$, could induce tumor necrosis or apoptosis by destroying cell homeostasis such as DNA damage and protein misfolding through acoustic cavitation-induced effects.[94] Nevertheless, US-mediated cell damage can be reversed and repaired accompanied by autophagy.[95] Thus, the autophagy inhibitor provides a potential therapeutic agent for enhancing tumor sensitivity and improving SDT efficacy. We recently found that nanosonosensitizer-mediated SDT was prone to induce pro-survival autophagy due to the increased ROS generation in breast cancer cells. The sequencing results displayed that the significantly altered genes mainly enriched in MAPK and AMPK autophagy-related signaling pathways. In view of this point, we developed a biocompatible nanoplatform PPIX/3-MA@Lip based on the rationally constructed nanoliposomes by encapsulating clinically approved sonosensitizer PPIX and classical autophagy inhibitor 3-methyladenine (3-MA) to optimize the SDT efficiency by augmenting autophagy inhibition[96] (Fig. 8(A)). Further studies demonstrated that PPIX-induced ROS destroyed the cellular homoeostasis and facilitated the autophagy sensitivity, thereby augmenting the efficiency of SDT-based synergistic therapy.

Owing to the heterogeneity in different types of cancer, the specific targeting moieties (mainly biotin, peptides, folic acid (FA), and antibodies) were modified onto the surfaces of NPs to construct a nanoplatform with targeting characteristics, realizing the efficient accumulation of NPs into tumor sites. For example, Zhao *et al.*[97] developed an enteric-coated granule titled as GMCDS-FA@CMC by coating carboxymethyl chitosan (CMC) on folic acid-modified phospholipid (SLB-FA) encapsulating mesoporous silicon-coated gold NPs loaded with chlorin (Ce6) and doxorubicin hydrochloride. The further studies demonstrated that GMCDS-FA@CMC could stimulate the specific release of Ce6 and DOX to the orthotopic colorectal tumor sites due to the targeting function of FA. The results showed that GMCDS-FA@CMC significantly enhanced the therapeutic effect and improved the prognosis *in vitro*. In short, GMCDS-FA@CMC as a multi-functional nanosystem provided a distinct strategy to achieve the efficient SDT-chemo combined therapy (Fig. 8(B)).

3.5.2 SDT combined with immunotherapy. Tumor immunotherapy is a therapeutic modality to control and eliminate tumors by restarting tumor-immunity cycle and resuming normal immune response. Unfortunately, recent studies have shown that most immunotherapy strategies have intrinsic limitations and disadvantages, including biosafety issues, off-

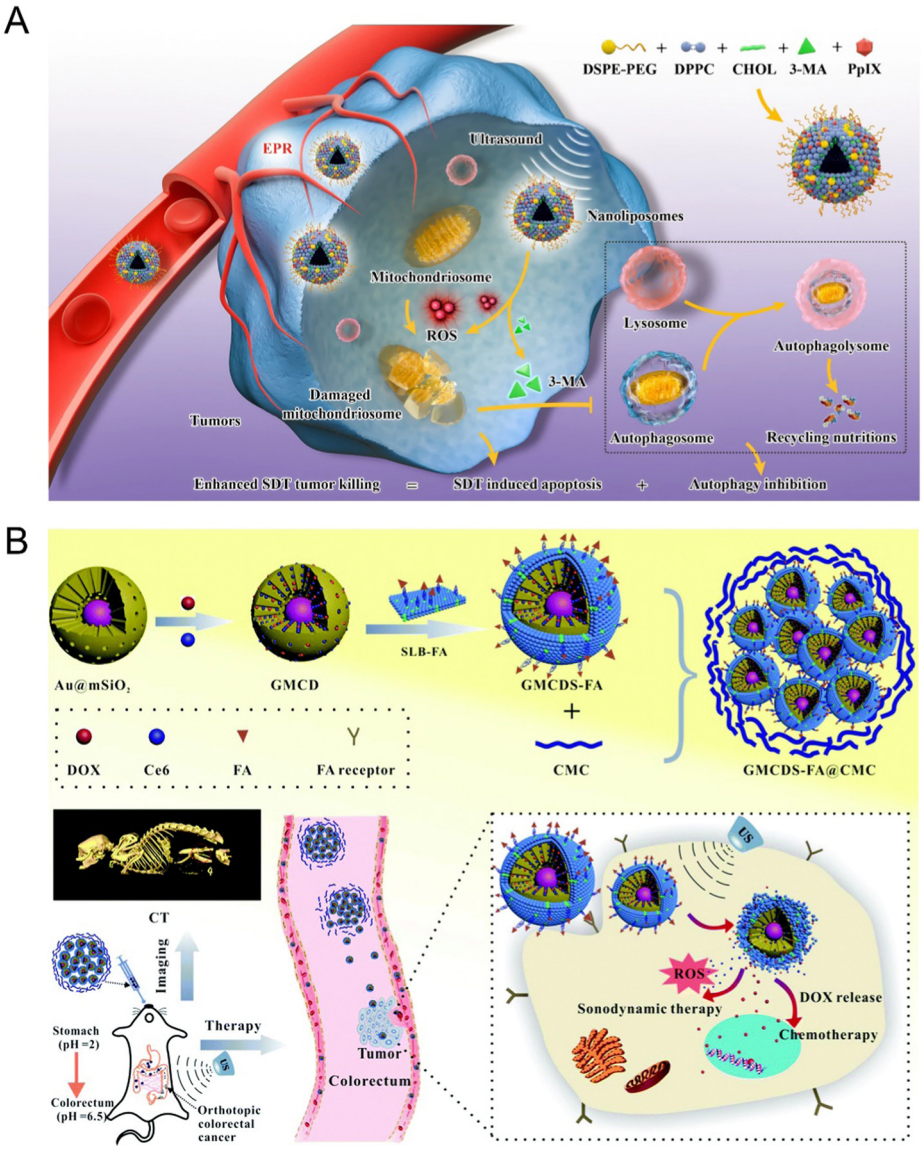

Fig. 8 (A) Schematic illustration of the synthetic procedure of PPIX/3-MA@Lip nanosonosentizer and the synergistic SDT and autophagy blockage process. Reproduced with permission.[96] Copyright 2021, Springer Nature. (B) Schematic illustration of the synthetic procedure of GMCDS-FA@CMC and the imaging and therapy processes. Reproduced with permission.[97] Copyright 2021, Royal Society of Chemistry.

target effects, inflammation, autoimmune reactions, and high costs. Recently, it has been reported that the fragments of tumor cells during SDT can serve as tumor antigens and activate the immunological system. However, the SDT-induced innate immune response alone is insufficient to inhibit the tumor recurrence and metastasis. Thus, the combination of SDT and immunotherapy is expected to be an efficient approach by enhancing the inherent immune response of SDT and suppressing the tumor growth.

In recent years, immune-checkpoint blockade therapy is becoming a key tool in the war against cancer. Immune checkpoints are immunosuppressive pathways that control immune response to preserve self-tolerance and safeguard neighboring tissues. Currently, several immune checkpoint agents, such as anti-PD-1 and anti-PD-L1, are clinically approved for cancer treatment.[98] However, the overall efficiency of checkpoint blockade immunotherapy is still unsatisfying due to the specific immunotoxicity. We recently developed a multifunctional nanosonosensitizer (HMME/R837@Lip) based on SDT combined with immune-checkpoint blockade.[99] All the components of HMME/R837@Lip are clinically approved and feature high biosafety. By employing multiple tumor models, we proved that the combination of HMME/R837@Lip with anti-PD-L1 not only significantly inhibited the growth of primary tumor but also enormously hindered the progress of lung metastasis *via* inducing systematic immune responses, including the rising of CD8+ and CD4+ effector T cells and the stimulated maturation of dendritic cells and cytokine secretion. Importantly, this combined treatment strategy also provided a durable immunological memory function, which was capable of preventing tumor recurrence (Fig. 9).

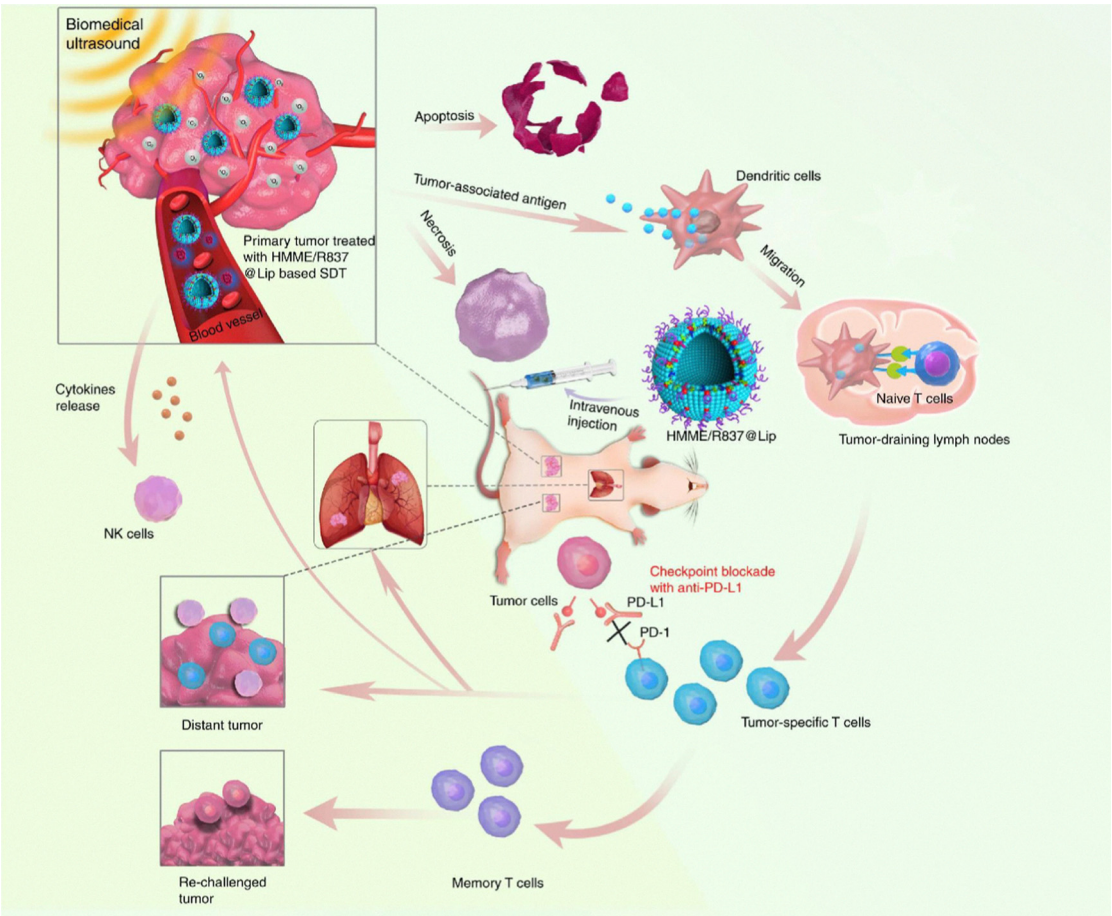

Fig. 9 Schematic illustration of HMME/R837@Lip-enhanced SDT combined with anti-PD-L1 for effective cancer immunotherapy. Reproduced with permission.[99] Copyright 2019, Springer Nature.

In addition to excellent therapeutic effects on malignant tumors, SDT combined with immunotherapy also featured remarkable antibacterial effects. *Methicillin-resistant staphylococcus aureus* (MRSA) is a highly drug-resistant bacterium, which has become the main pathogen of nosocomial infection, mainly found in patients with long-term chronic diseases who need to use antibiotics repeatedly and also often seen in patients in intensive care units. At present, both traditional antibiotic treatment and proactive vaccine prevention are unable to effectively control MRSA infection. For example, Niu *et al.*[100] developed M2 macrophage membranes-coated PLGA NPs with IR780 encapsulation (M2/IR780@PLGA) to improve the therapeutic efficacy of MRSA myositis through combining SDT with anti-infection immune response. M2/IR780@PLGA NPs notably reduced the expression of CD86 and significantly raised the levels of CD206 and IL-10, indicating the inhibition of M1-type macrophages and the conversion of M1-to-M2 macrophages. In addition, a large quantity of M2/IR780@PLGA NPs was found to accumulate at the inflammation sites in the MRSA-infected mouse models owing to the coating of M2 macrophage. Meanwhile, the lower blood flow signals and a mild edema were also observed in the M2/IR780@PLGA NP-based SDT group under HIFU imaging guidance. Furthermore, the histopathology test revealed that the infected legs in the M2/IR780@PLGA-mediated SDT group had slighter bacterial penetration, increased M2 macrophage and reduced M1 macrophage and the higher percentage of mature dendritic cells in spleen, demonstrating that M2/IR780@PLGA NPs could effectively boost the antibacterial SDT and promote M2 macrophage polarization to enhance the therapeutic efficacy of MRSA myositis.

3.5.3 SDT combined with PDT. PDT is considered to be one of the effective therapies for cancer and various nonmalignant diseases due to its advantages of high controllability, physical targeting, non-invasiveness and low side effects. PDT works by irradiating the lesion location with light and activating photosensitizers (PSs), inducing the luminous chemical reaction and producing ROS to eliminate pathological cells. However, the low light penetration depth (0.5–2.0 mm), poor transfer efficiency of PSs and oxygen-dependent nature substantially restrict its further clinical application.[101] With the gradual development of nanotechnology, some nanocomposites have been confirmed to simultaneously exert therapeutic effects of PDT and SDT and generate a large amount of ROS, thus decreasing the sensitizer dose and amplifying the cytotoxicity. This new-fashioned treatment modality is referred to as sonophotodynamic therapy (SPDT).

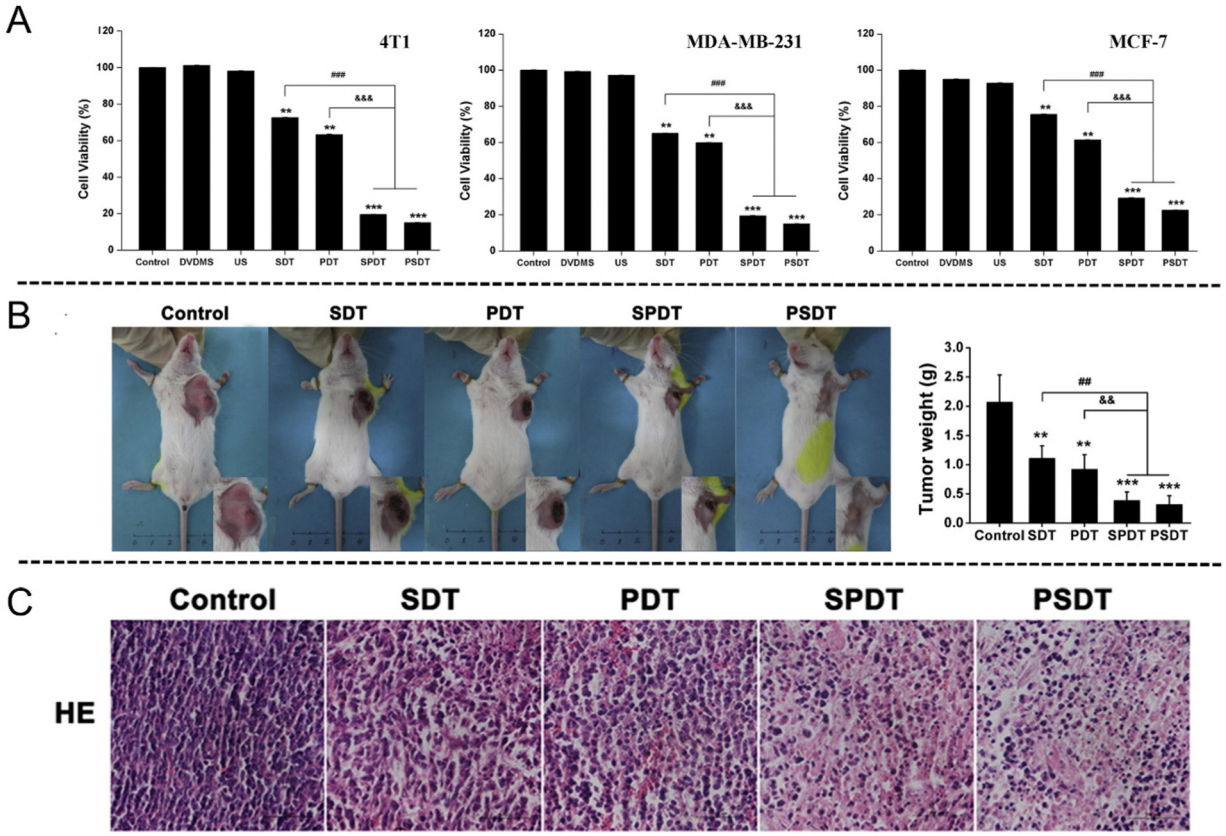

Fig. 10 (A) *In vitro* cytotoxicity assessment of DVDMS-SPDT on 4T1, MDA-MB-231 and MCF-7 cells determined by MTT assay. Error bars represent the SD from three independent experiments. $^{**}p < 0.01$ *versus* control, $^{***}p < 0.001$ *versus* control, $^{\#\#\#}p < 0.001$ SPDT/PSDT group *versus* SDT group, and $^{\&\&\&}p < 0.001$ SPDT/PSDT group *versus* PDT group. (B) Tumor weight of tumor-bearing mice after different treatments. Error bars represent the SD from three independent experiments. $^{**}p < 0.01$ *versus* control, $^{***}p < 0.001$ *versus* control, $^{\#\#}p < 0.01$ SPDT/PSDT group *versus* SDT group, and $^{\&\&}p < 0.01$ SPDT/PSDT group *versus* PDT group. (C) Tumor sections stained with hematoxylin and eosin (H&E) after different treatments. Reproduced with permission.[102] Copyright 2016, Elsevier.

As a newly discovered sensitizer, sinoporphyrin sodium (DVDMS) is a conjugation of two porphyrin monomers derived from photofrin II. Wang *et al.*[102] assessed the tumor inhibition effects of SDT and PDT on breast cancer by using DVDMS both *in vitro* and *in vivo*. The *in vitro* results showed that the cell (4T1, MDA-MB-231 and MCF-7 cell lines) viabilities decreased obviously in the combined treatment groups with addition of 0.5 μM DVDMS for 24 h, affirming the DVDMS-mediated SPDT therapeutic effect (Fig. 10(A)). The tumor volume and weight of mice in SPDT group were markedly suppressed comparing with single-modality treatment group (Fig. 10(B)). In addition, histopathological analysis exhibited that the tumor tissue was destructed in a large scale following SPDT treatment (Fig. 10(C)).

Rose Bengal (RB) is a red-emitting fluorescent dye that is broadly applied as a photosensitizer for anti-cancer and anti-bacterial PDT due to its ROS generation capacity.[103] However, its high aqueous solubility and poor bioavailability necessitated the development of new RB derivatives (RBDs). Huang *et al.*[104] designed and fabricated six new RB derivatives (RBDs) containing appropriate privileged moieties, aiming to optimize the amphiphilic properties. Among them, RBD4 significantly improved cellular uptake and enhanced intracellular ROS generation efficiency upon light and US irradiation, resulting in the remarkable anticancer potency. Methoxypolyethylene glycol moiety-appended RBD4 dramatically increased the cellular uptake and improved the ROS production efficiency in HepG2 cells under the combined irradiation of US and UV, which provided a possibility for RB as a potential anticancer drug in SPDT.

3.5.4 SDT combined with PTT. PTT is a well-known non-invasive phototherapy that uses photothermal agents (PTAs) to convert light energy into heat energy and kill tumor cells under near infrared (NIR) or other external light sources. Recently, PTT has shown great potential in the field of tumor ablation because of its simplicity, safety, remote control and non-invasiveness. However, the limited light penetration depth and low delivery efficiency of PTAs are also the main challenges in clinical development of PTT. Considering the high tissue penetration depth of US, the combination therapy of SDT and PTT is regarded as an efficient SDT-based synergistic therapeutic modality.

For instance, Lin *et al.*[105] fabricated a well-designed Pt–CuS Janus nanostructure consisting of a hollow CuS semiconductor and noble metal Pt. Due to the enhancement of local electric field, the deposition of Pt not only enhanced the hot electron generation but also enabled the catalytic decomposition of

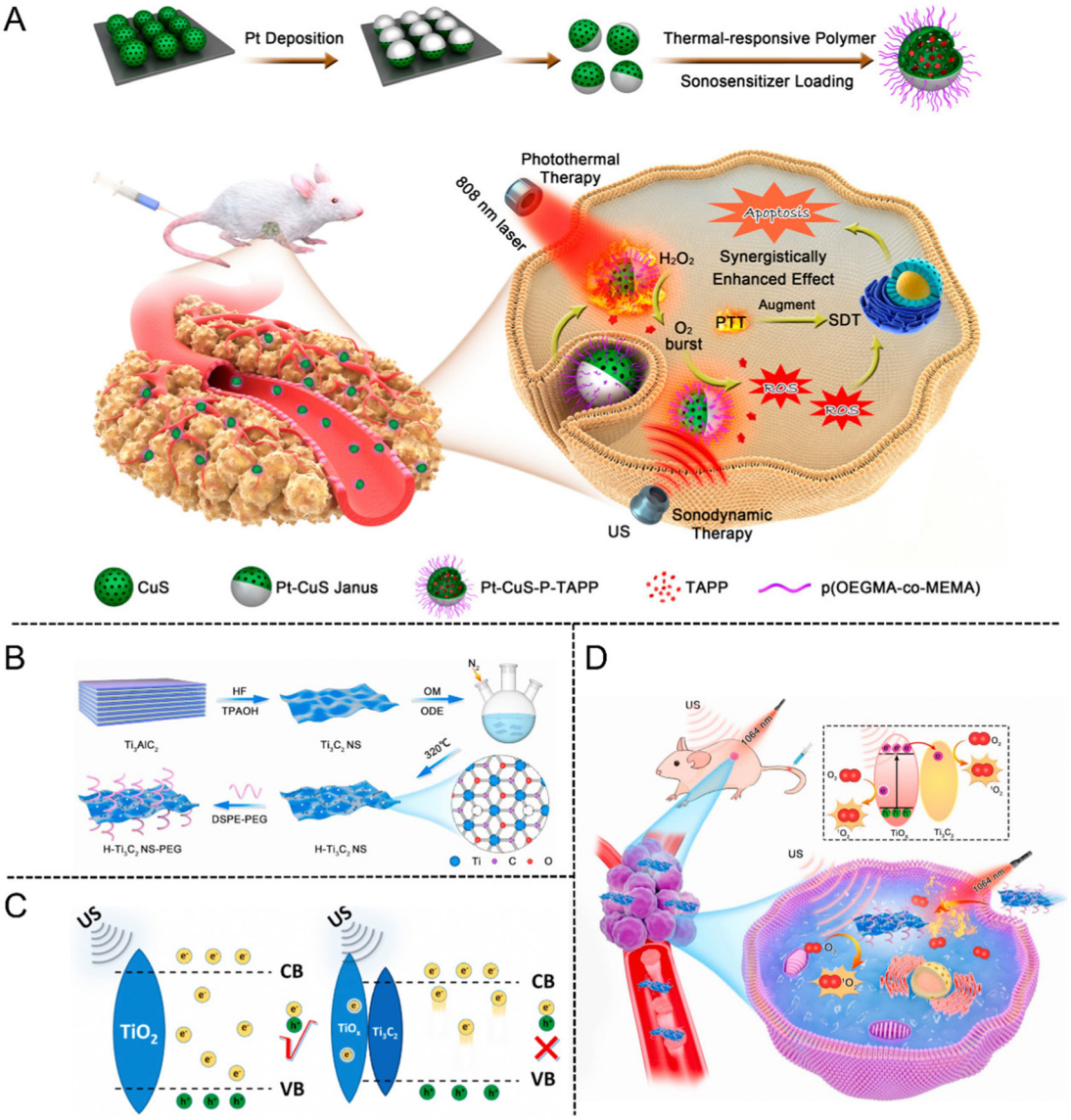

Fig. 11 (A) Schematic illustration of the synthesis procedure of PCPT and PCPT-mediated synergistic SDT/PDT cancer therapy. Reproduced with permission.[105] Copyright 2019, American Chemical Society. (B) Schematic of the preparation process of H-Ti_3C_2 NSs. (C) The action mechanism of TiO_2 NPs and H-Ti_3C_2-PEG NSs under US irradiation. (D) Schematic illustration of H-Ti_3C_2-PEG NSs for photothermal-enhanced sonodynamic therapy. Reproduced with permission.[106] Copyright 2022, Elsevier.

intracellular H_2O_2, further facilitating the ROS production to eradicate tumor cells. Interestingly, after coating the thermally sensitive copolymer p(OEGMA-*co*-MEMA) and loading TAPP molecules into the hollow interior of CuS (Pt-CuS-P-TAPP, labeled as PCPT), the catalytic activity of Pt and the release rate of PAPP were regulated in real time according to the temperature change. Additionally, the synergistic effect of SDT and PTT mediated by PCPT exhibited complete tumor elimination with no evidence of recurrence and featured an excellent therapeutic biosafety (Fig. 11(A)).

MXenes are a new type of 2D transition metal carbides, nitrides or carbonitrides, which are single-layer or several-layer nanosheets obtained by stripping the $M_{n+1}AXn$ phase material (MAX phase). The unique 2D layered structure, large specific surface area, excellent conductivity and mechanical stability have enabled MXenes to rapidly become a research hotspot in biomedicine. Cheng *et al.*[106] fabricated a new type of oxygen-defective Ti_3C_2 nanosheets (H-Ti_3C_2 NSs) derived from MXenes by two-step methods of chemical exfoliation and high-temperature treatment (Fig. 11(B)). The increased oxygen defect of H-Ti_3C_2 NSs emerged after treating with high temperature. The electrons and holes could split more quickly as the oxidation level increased under US irradiation, meanwhile, sufficient oxygen defects could prevent electron–hole recombination (Fig. 11(C)). By comparison with Ti_3C_2 NSs without high-temperature treatment, the sonodynamic efficiency of H-Ti_3C_2 NSs was significantly increased by 3.7 times. After modifying H-Ti_3C_2 NSs with the amphiphilic polymer of DSPE-PEG (2000),

the stability and biocompatibility of H-Ti_3C_2-PEG NSs were significantly improved. *In vitro* studies demonstrated that the mild photothermal effect could facilitate the endocytosis of H-Ti_3C_2-PEG NSs for enhancing the SDT efficiency. Further evidence came from *in vivo* investigations, which revealed that the mild photothermal impact could significantly increase the SDT effect by reducing the oxygen deficit in the TME (Fig. 11(D)).

3.5.5 SDT combined with CDT. CDT is a novel anti-tumor therapeutic strategy, which takes advantage of the weak acidic environment and the high concentration of H_2O_2 at the tumor site to generate Fenton or Fenton-like reaction, thereby catalyzing endogenous H_2O_2 to generate $^{\bullet}OH$.[107–109] $^{\bullet}OH$ as the most lethal reactive oxygen species in the biological system could kill tumor cells by destroying biological macromolecules such as lipids, proteins and DNA. Fenton or Fenton-like reaction efficiency highly depends on the selection of transition metal ions. To date. a large number of Fe-, Cu-, and Mn-based CDT nanodrugs have been widely developed.[110–112]

Although CDT has been widely explored and studied in recent years, there are still some limitations in the clinical application due to its poor therapeutic effect. It is mainly challenged by the following three aspects: (1) the relatively high pH value of the tumor site is not suitable for Fenton/Fenton-like reactions; (2) the low endogenous H_2O_2 concentration is not sufficient to produce $^{\bullet}OH$ continuously; (3) the high expression of reduced substances (such as glutathione) in tumor microenvironment weakens the therapeutic effect of CDT. Accordingly, CDT combined with other treatment methods, such as SDT, can help to make up for the shortcomings of single therapy, so as to achieve synergistic and efficient tumor treatment.[107] For example, Cheng *et al.*[113] reported a new type of biodegradable iron-doped vanadium disulfide nanosheets (Fe–VS_2 NSs) modified with PEG for SDT due to the extended electron–hole recombination time. Furthermore, Fe–VS_2-PEG NSs were used as a typical Fenton agent to promote chemodynamic therapy (CDT) by catalyzing the intracellular H_2O_2 within the tumor microenvironment. Simultaneously, Fe and V as multivalent metal ions in the Fe–VS_2 NSs increased the consumption of glutathione to magnify the ROS-induced oxidative stress mediated by SDT combined with CDT (Fig. 12(A)). Furthermore, Zhang *et al.*[114] synthesized novel hypoxia-responsive metal–organic framework nanoparticles loaded with sonosensitizer Ce6 (Cu-MOF/Ce6 NPs) for SDT combined with CDT through precise delivery of drugs. The large size Cu-MOF/Ce6 can effectively accumulate in the tumor through EPR and decompose in response to the anoxic TME to release $Cu^{2+}$and Ce6. Endogenous Cu^{2+} combines with nearby GSH to deplete it and turn it into Cu^{+}, which then reacts with internal H_2O_2 to produce $^{\bullet}OH$ *via* a Fenton-like process for CDT. The synergistic effect of SDT and CDT is significantly enhanced due to the decrease of GSH content, which can kill MCF-7 tumor cells with minimal invasiveness and specificity (Fig. 12(B)).

3.5.6 SDT combined with nanozyme-catalyzed therapy. Nanozymes are a kind of artificial nanomaterial with enzyme-like catalytic activity, including metals, metal oxides, metal coordination compounds, carbon nanomaterials, polymers and so on.[115] It has some similarities with natural enzymes in terms of overall size, shape and surface charge, thus simulating the catalytic activity of natural enzymes. Most natural enzymes composed of proteins are easy to inactivate and lose catalytic activity when encountering high temperature, strong acid, strong base and other environments. Compared with natural enzymes, nanozymes have been widely used in the biomedical field due to the advantages of low preparation cost, high yield, stability and easy storage.[116]

Nanozyme-catalyzed therapy is a potential tumor treatment method, which uses nanostructures with natural enzyme-like catalytic activity to produce ROS in the tumor microenvironment.[117] The application of traditional sonosensitizers in clinic is usually limited as a result of their poor water solubility, tendency to aggregate under physiological conditions, and low bioavailability. In addition, most of the sonosensitizers can only produce a large number of ROS under US radiation in the presence of O_2, so the hypoxic environment of tumor tissue is not conducive to SDT in many cases. However, the emergence and development of nanozyme-catalyzed therapy provide a possibility to solve the limitations of SDT against cancer. For example, Liu *et al.*[118] developed a cascade nanozyme (HABT-C) with multienzyme-mimic activity for SDT combined with nanozyme-catalyzed therapy to achieve the reversal of tumor immunosuppression and alleviate hypoxia in the tumor microenvironment. Firstly, the hollow white titanium dioxide with sodium borohydride has been reduced to obtain black titanium dioxide. Subsequently, they deposited gold on the surface of black titanium dioxide and sintered it in hydrogen (HABT). Finally, HABT was further functionalized by using carbon nanodots and hyaluronic acid to produce cascade nanozymes with targeted function (HABT-C@HA). The structure characterization showed that HABT-C@HA with a mesoporous structure can improve the formation conditions of the cavity and the transport of ROS. Above all, HABT-C@HA possesses multienzyme-mimic activities, including glucose oxidase-, catalase- and peroxidase-mimicking activities, and undertakes the dominant therapeutic task, including the cutoff of tumor energy, the reversal of hypoxic microenvironment, and continuous output of ROS. Both *in vitro* and *in vivo* experiments showed that the cascade reaction triggered by HABT-C@HA can enhance the ROS production under US radiation and synergistically magnify the therapeutic effect of SDT (Fig. 13).

3.5.7 SDT combined with gas therapy. Gas molecules such as nitric oxide (NO), hydrogen (H_2), carbon monoxide (CO), oxygen, hydrogen sulfide (H_2S) and sulfur dioxide (SO_2) are capable of regulating various physiological functions, including nervous system, cardiovascular system and immune system, which play an important role in the normal operation of human physiological processes and active regulation of pathological processes.[119,120] In addition, the adjustment of gas concentration in TME can affect the Wahlberg effect, thereby inhibiting the proliferation process and accelerating the cell apoptosis, while the activity and physiological function of normal cells are not affected.[121] Therefore, gas therapy has been developed as a safe and effective "green" cancer treatment.[122] However, uncontrolled gas ingestion or release would bring potential poisoning risks and

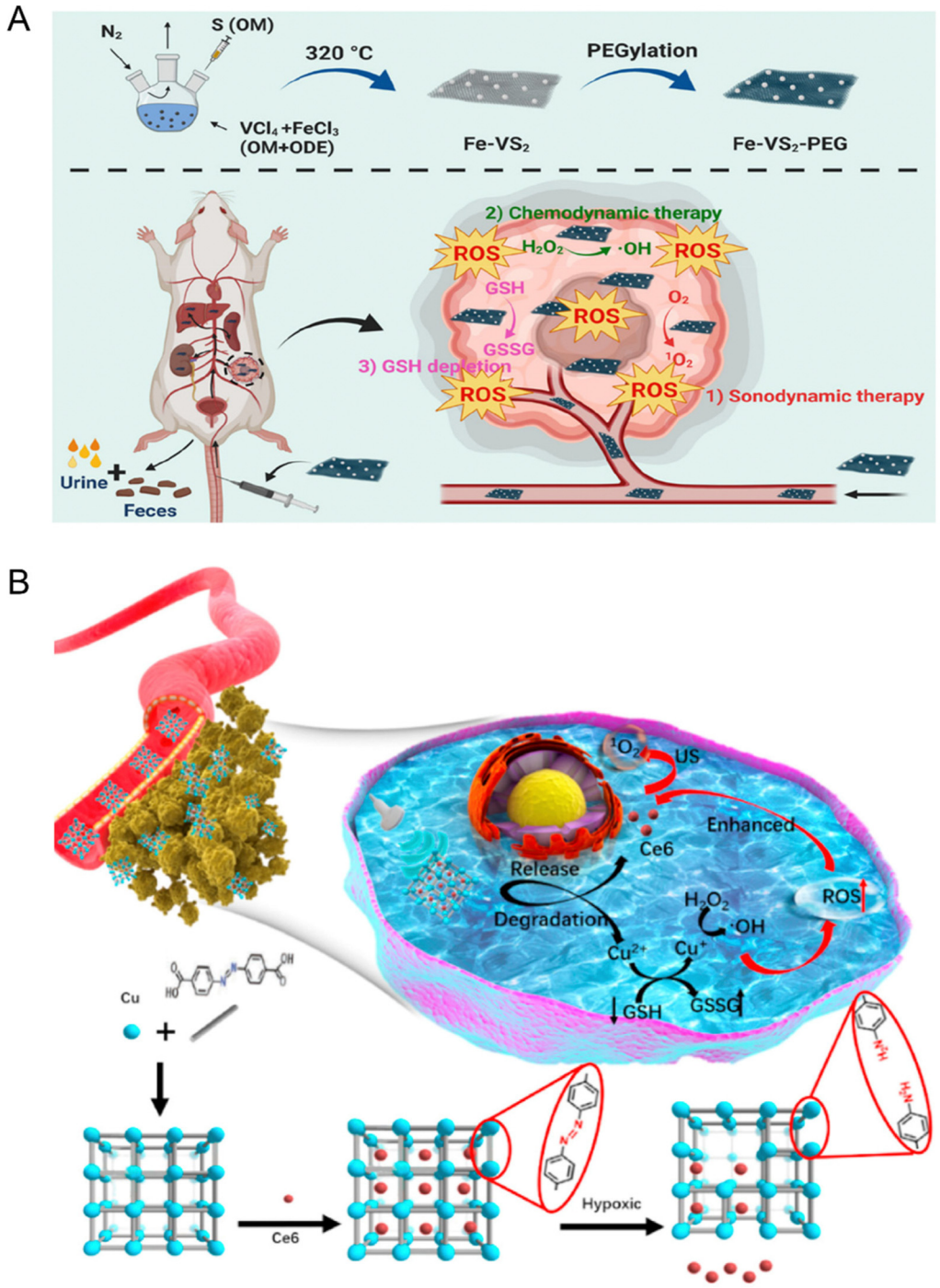

Fig. 12 (A) Schematic diagram of Fe–VS_2 NSs synthesis and bioapplication in the combined cancer therapy. Reproduced with permission.[113] Copyright 2020, American Chemical Society. (B) Schematic illustration of the synthetic procedure and hypoxia-responsive copper metal–organic framework nanosystems for improved cancer therapy. Reproduced with permission.[114] Copyright 2020, Elsevier.

decrease the therapeutic effects. Combining SDT with gas therapy has been exploited as a potential strategy to control gas release for enhancing cavitation effect of SDT.

Wang *et al.*[123] prepared mesoporous titanium dioxide nanosystems (T-mTNPs@L-Arg) by loading NO donor precursor L-arginine (L-Arg) and modifying the surface with mitochondria-targeting ligand triphenyl phosphine (TPP). Owing to the TPP modification, the T-mTNPs@L-Arg could be ingested through the cytoplasm and target mitochondria, which generated large amounts of ROS to induce mitochondrion damage under US irradiation. In addition, T-mTNPs@L-Arg enabled L-arginine release *via* pH response and produced NO gas in the H_2O_2-enriched TME. NO has been proved to restrain mitochondrial complex IV through competitively binding with the O_2 binding

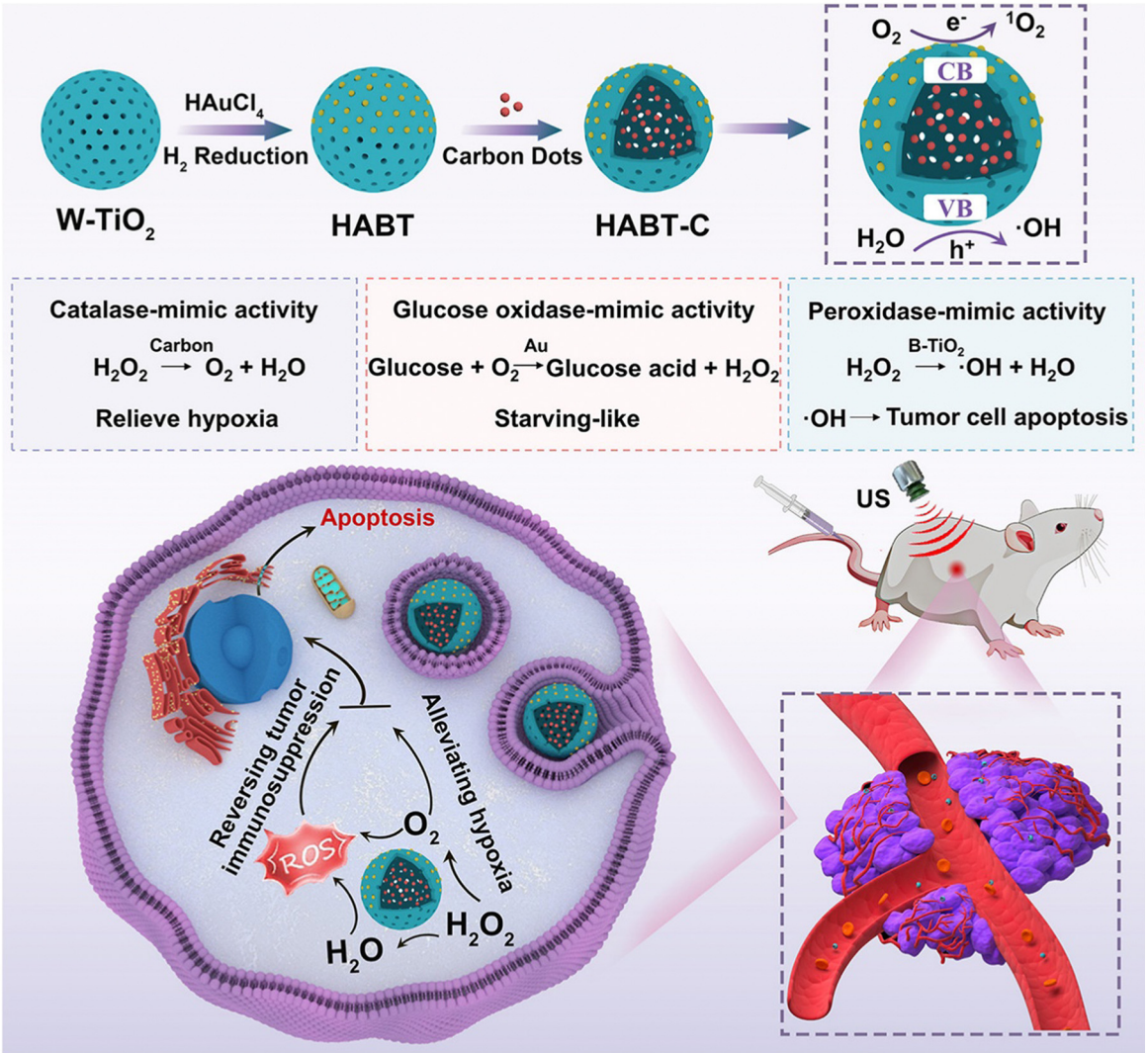

Fig. 13 Schematic Illustration of synthesis and antitumor therapy of HABT-C@HA. Reproduced with permission.[118] Copyright 2022, American Chemical Society.

sites of cytochrome *c* oxidase (Cco) for inhibiting the hyperactive metabolism of O_2. In view of mitochondria-targeting ability and NO release, the T-mTNPs@L-Arg could not only facilitate more lethal reactive nitrogen species (RNS) generation, but also mitigate the hypoxia status of TME. The engineered T-mTNPs@L-Arg also featured high biocompatibility and biosafety (Fig. 14(A)).

Likewise, Gu *et al.*[124] fabricated a stimuli-responsive anethole dithiolethione (ADT)-loaded magnetic nanoliposome (AML) delivery system, which was composed of hydrogen sulfide (H_2S) pro-drug ADT, a phospholipid shell, and superparamagnetic NPs. The H_2S mapping in HepG2 tumor cells and Prussian blue staining indicated that AMLs could generate H_2S bubbles and induce tumor cell death. The nanosized AMLs could intratumorally turn into massive micron scale H_2S bubbles after applying an external magnetic field and magnetic resonance and US dual modal imaging were capable of monitoring this dynamic process in real time. Additionally, the break of intra-tumoral H_2S bubbles could cause the ablation of tumor tissues during exposure of higher acoustic intensity. Meanwhile, intra-tumorally enhanced H_2S molecules entered the internal tumor region as gasotransmitters to further demonstrate synergistic anticancer effects and prevent metastasis (Fig. 14(B)). To sum up, as multimodal therapeutic agents, the AMLs not only displayed an enhanced therapeutic effect on tumors but also facilitated US-guided imaging.

4. US-related therapeutic mechanisms

There have been a lot of studies on the potential mechanism of US-related therapy *in vitro* and *in vivo*, but the exact mechanism remains to be clarified due to the complexity of the US-related therapy process. Up to now, most research supports that US-related therapy produces a synergistic effect to cause cell death through multiple mechanisms, including US cavitation effect, ROS effect and US-induced apoptosis.[13] Nevertheless, the

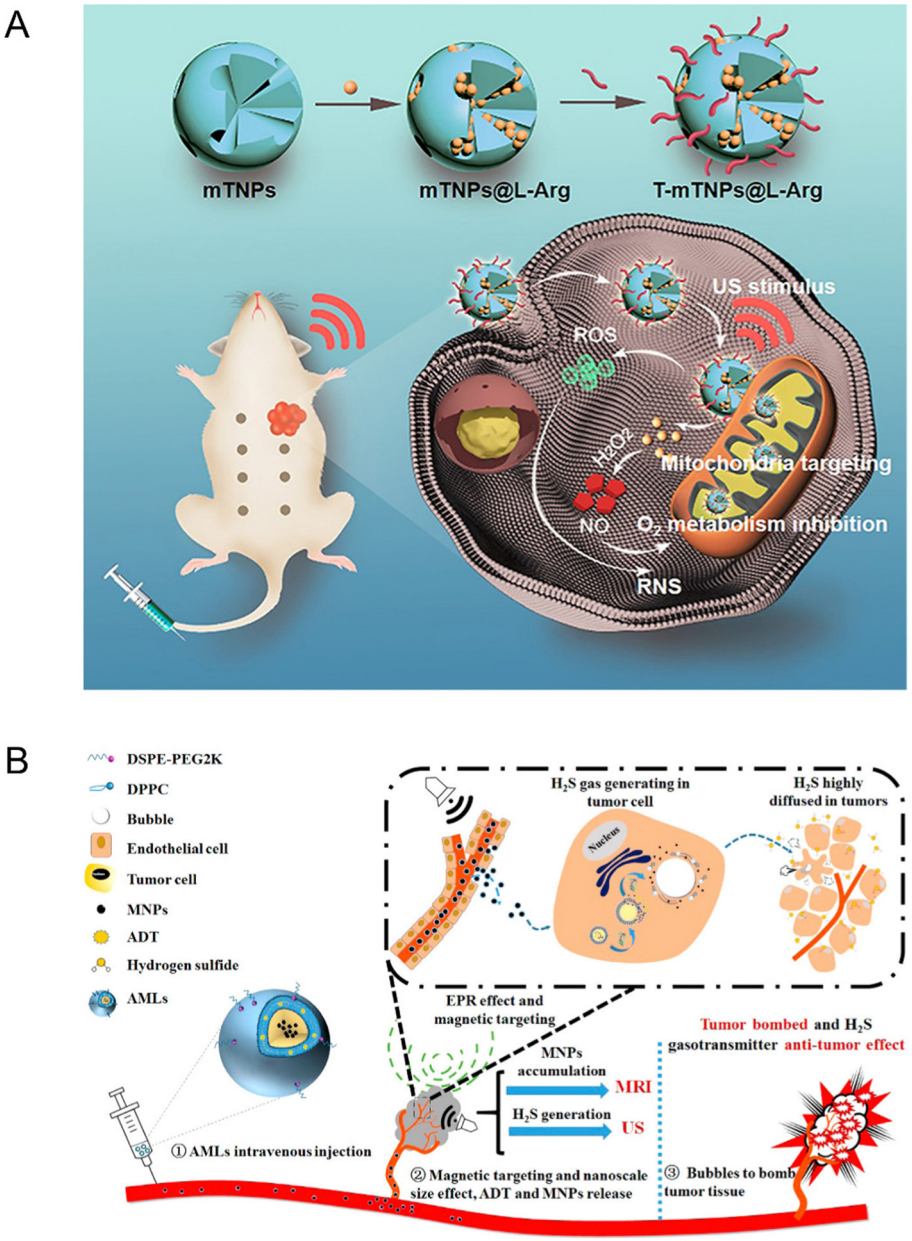

Fig. 14 (A) Schematic illustration of T-mTNPs@L-Arg for synergistic nitric oxide gas-sonodynamic therapy. Reproduced with permission.[123] Copyright 2022, Dove Medical Press. (B) Schematic illustration of AMLs and the nano-micro conversion process for synergistic H_2S gas-sonodynamic therapy. Reproduced with permission.[124] Copyright 2017, American Chemical Society.

verification of the definitive mechanism of US-related therapy needs more evidence.

4.1 Cavitation effect

The ultrasonic cavitation technology has shown high application potential in the field of clinical treatment such as in thrombolytic therapy, hemostasis therapy, tumor therapy, real-time acquisition of cavitation images, gene expression and drug delivery. The ultrasonic cavitation effect is a special physical phenomenon, which means that the mechanical pressure of tissue fluid increases rapidly under the action of US, resulting in the formation of a large number of cavitation MBs with a diameter of 1 to 10 μM. Under the action of US with a certain intensity and frequency, cavitation MBs would vibrate, expand and even burst, resulting in the collapse of cell membranes and increased permeability. Generally speaking, ultrasonic cavitation can be divided into two types: non-inertial cavitation and inertial cavitation. The former refers to the continuous oscillation in a small range of cavitation MBs caused by low intensity US, thus enhancing the outward diffusion rate of core gas. The latter refers to the rapid expansion and contraction of cavitation MBs caused by high-intensity US and a large number of MBs break in a short time, resulting in strong shock waves and local high temperature and pressure. This violent physicochemical reaction can result in

tissue damage, which is manifested by significantly enhancing the permeability of cell membrane, inducing endothelial cell gap widening, DNA breakage, and ultimately leading to microvascular rupture, hemolysis, bleeding and thrombosis. Regardless of the type, the final result is conducive to the intercellular drug transport, so as to improve the therapeutic effect of SDT on tumors.

The cavitation effect is a threshold effect, which is closely related to the existence, quantity and concentration of MBs in liquid. The MB contrast agent, as an artificial cavitation nucleus, can significantly enhance the cavitation effect. The main mechanisms are as follows: the increase of exogenous cavitation nuclei and the reduction of ultrasonic cavitation threshold. The existence of MBs can reduce the total energy required to generate cavitation and reduce the energy threshold causing cavitation effect. Therefore, the controllable cavitation effect produced by US combined with MBs has broad prospects in the field of clinical treatment. Additionally, cavitation can induce sonoluminescence (SL) effect and sonoporation effect. The SL effect refers to the process where MBs emit light when squeezed by ultrasonic waves in liquid. SL can excite the electron orbit of the sonosensitizer through energy transfer and generates ROS when the excited electrons return to the ground state.[125,126] The excess ROS will accumulate in the cytoplasm and organelles to destroy proteins, DNA and promote lipid peroxidation, eventually leading to cell death.

Sonoporation is a mechanical effect caused by the oscillation of cavitation MBs near the cell membrane under US irradiation with the certain intensity and frequency. This mechanical oscillation can produce a large number of transient micropores on the surface of the cell membrane. The half-life of the micropores is about 10 minutes and the diameter of the micropore ranges from several nanometers to 150 nanometers. Hence, the sonoporation effect can increase the permeability of microvascular endothelial cells and enhance the absorption and transportation of drugs, which enables drugs to continuously reach effective blood concentration in cells and tissues.[127,128] For instance, Callan *et al.*[129] showed that the inhibitory effect of DOX and taxol on tumor cells was significantly improved after US irradiation, which may be due to the improvement of drug uptake efficiency by sonoporation effect. In addition, low intensity US can stabilize the production of cavitation MBs, so that they can enter tumor cells more easily. Owing to this characteristic, low intensity US is an ideal selection for producing sonoporation effect. However, it is worth noting that low-frequency US, as one of the inducing factors of cell self-repair, can increase the cell oxygen content by improving the permeability of blood vessel walls and cell membranes, which is beneficial to the growth of tumor cells. Therefore, SDT must be used in conjunction with anticancer medications for treating malignant tumors.

4.2 ROS effect

ROS is a class of oxygen-containing atoms or atomic groups with active chemical properties, including $^1O_2$, the superoxide anion (O_2^-), and $^\bullet OH$.[108] The ROS generation induced by SDT is mainly achieved through two approaches. On the one hand, the sonosensitizer can be activated from the ground state to the excited state and directly react with surrounding oxygen molecules or other substrate molecules to form free radicals under the action of ultrasonic cavitation. In addition, it will release energy when returning to the ground state and the released energy can interact with surrounding oxygen molecules, resulting in the $^1O_2$ production. On the other hand, the ultrasonic cavitation effect activates the sonosensitizers inside or near the cavitation bubble and leads to ROS production through pyrolysis of water at high-temperature.

$^1O_2$ is considered as the main medium of sonodynamic activity with the strong oxidation capacity, leading to irreversible damage of targeted pathological cells and directly mediating cytotoxicity. In addition, hydrogen peroxide and the superoxide anion can also induce cell damage or apoptosis through the chain reaction mechanism of lipid peroxidation. Excessive ROS will not only lead to oxidative stress and damage, but also cause cytoskeleton contraction, chromatin concentration and DNA fragmentation and ultimately lead to apoptosis.[130]

Theoretically, there are two ways to destruct the redox balance *in vivo* and cause cell death. One method is to increase the ROS concentration by promoting the ROS production and the other method is to inhibit the clearance of ROS. Several studies have shown that specific ROS scavengers such as histidine, mannitol and superoxide dismutase (SOD) can prevent tumor cells from being destroyed by SDT, providing a theoretical basis for the effect of ROS.[131] Hence, utilizing the ROS generation mechanism of SDT to improve the therapeutic efficiency of SDT is a potential cancer-therapeutic modality.

4.3 Piezoelectric effect

The piezoelectric effect was discovered by Pierre Curie and Jacques Curie in 1880.[132] When the piezoelectric semiconductor bears the external stress, the crystal will be polarized, thus inducing the formation of piezoelectric charge (bound charge) and piezoelectric potential with opposite signs at both ends, namely, the piezoelectric effect.[133] Under the action of mechanical vibration, positive and negative charges will accumulate on the surface of piezoelectric semiconductor materials and lead to catalytic reactions, which is known as piezoelectric catalysis. In recent years, piezoelectric nanomaterials have also been explored as sonosensitizers for SDT and used in tumor therapy[134] and antibacterial therapy.[135] Nanomaterials with small volumes and large surface areas are conducive to rapid charge transfer between the catalyst and redox dipole, achieving high catalytic activity.[136] US with excellent spatiotemporal control ability can be used as a source of mechanical force for piezoelectric nanomaterials.[137] Therefore, combining US and piezoelectric catalysis is a promising and potential therapeutic approach.

Photocatalysis refers to the participation of photo-induced charges (electron–hole pairs) in catalytic redox reactions.[138] Similar to the photocatalysis process, piezoelectric charges induced by mechanical vibration can also be used to drive catalytic redox reactions. On the surface of the polarized piezoelectric materials, the bound and shielding charges are in equilibrium, so the material is electrically neutral as a whole. Under the action of US with a certain frequency and intensity,

MBs break and release ultra-high pressure (up to 108 MPa) around them, which is applied to nearby piezoelectric materials. At this time, the compressive stress (negative strain) based on the piezoelectric effect reduces the polarization strength of the material, causing the charge carriers to redistribute on its surface and releasing redundant shielding charges from the material surface. Subsequently, the excessive shielding charge is dispersed into the surrounding solution to form a free charge, which reacts with H_2O or O_2 in the environment to produce $^{\bullet}OH$ or O_2^-.[139,140] The surface of the material absorbs the surrounding free charge to supplement the shielding charge and balance the bound charge produced by the piezoelectric effect when the applied compressive stress lowers (positive strain). At the same time, the charge in the electrolyte with opposite polarity to the adsorbed charge will participate in the redox reaction again and continuously generate ROS. Therefore, piezoelectric nanomaterials in alternating stress and electrolyte environments can constantly provide charge to generate $^{\bullet}OH$ or O_2^- for the application of relevant fields.

4.4 US-induced apoptosis

Apoptosis refers to the active and orderly cell death caused by gene regulation in order to maintain the homeostasis of the internal environment under physiological or pathological conditions. It is also called ''programmed cell death'' in medicine. Cells in the apoptosis process are usually characterized by cytoskeleton contraction, chromatin concentration, DNA breakage and caspase activation. It has been reported that SDT can damage mitochondria and then release cytochrome *C* (cyt-*c*) to activate caspases.[141] Caspases can hydrolyze many key enzymes in cells, such as poly ADP-ribose polymerase (PARP), which can repair some mutations and damages of DNA. At the same time, the mitochondrial damage caused by SDT can reduce the oxygen supply of cells and promote tumor cell apoptosis. Leung *et al.* reported that SDT can mediate apoptosis of leukemia cells and its mechanisms involve mitochondrial damage, DNA breakage, cytoskeleton changes, ROS production and autophagy. Normal red blood cells and white blood cells, however, are not harmed under the same circumstances. This difference may be due to the regulation of p53, changes in signal pathways, and the enhancement of cellular tolerance to oxidative stress.[142]

SDT can also induce the expression of the B-cell lymphoma/leukemia-2 (Bcl-2) gene family and its associated x gene (Bcl-2 associated X, Bax). Cao *et al.*[143] evaluated the antitumor effect of DVDMS-mediated SDT (DVDMS-SDT) on hepatocellular carcinoma *in vitro* and *in vivo*. The results showed that DVDMS-SDT increased the proportion of cells in G2/M phase and decreased the levels of cyclin-dependent kinase 1 (CDK1) and cyclin B1 proteins. The generated ROS increased the expression of p53 and Bax and decreased the expression of Bcl-2. Concurrently, ROS generation led to the activation of caspase-3 and finally induced apoptosis.

Furthermore, SDT can induce apoptosis through overload of calcium ions (Ca^{2+}) in the mitochondrial membrane. Li *et al.*[144] studied the apoptosis mechanism of C6 glioma cells induced by SDT mediated by hematoporphyrin monomethyl ether (HMME). The data demonstrated that C6 glioma cells treated with SDT revealed an increased level of ROS production, decreased mitochondrial membrane potential (MMP) and an enhanced release of cyt-*c*, indicating the cell apoptosis process. In addition, this apoptotic effect was found to be correlated with the overloaded Ca^{2+}, derived from the intra- and extracellular sources in the early apoptotic process.

5. Conclusions and perspectives

With the vigorous development of nanomedicine and materdicine, the development and optimization of new types of

Table 1 Summary of various sonosensitizer types for biomedical applications

Category	Materials	US parameters	Biological models	Ref.
Traditional sonosensitizer	HP	1.92 MHz, 3.18 W cm^{-2}, 60 s	Sarcoma 180 cells	15
	PPIX	2.2 MHz, 3.0 W cm^{-2}, 30 s	Sarcoma 180 cells	17
	HMME	10.5 MHz, 0.5 W cm^{-2}, 10 s	UMR-106 cells	19
	Pcs	1.0 MHz, 2.44 W cm^{-2}, 5 min	Nucleated erythrocytes	19
	RB	1.93 MHz, 5.9 W cm^{-2}, 60 s	Sarcoma 180 cells	21
	DOX	1.0 MHz, 0.5 W cm^{-2}, 60 s	U937 cells	24
Titanium dioxide nanomaterials	TiO_2	1 MHz, 1.0 W cm^{-2}, 2 min	C32 cells	26
	PEG-TiO_{1+x}	40 kHz, 3.0 W cm^{-2}, 50% duty cycle, 5 min	4T1 cells	27
	W-TiO_2	None	143B cells	28
	GFP-TiO_2	1 MHz, 1.0 W cm^{-2}, 120 s	HepG2 cells	29
Noble metal nanomaterials	Au@Cu_2O	1 MHz, 1.5 W cm^{-2}, 50% duty cycle,15 min	*S. aureus.*	30
	Au–TiO_2	1.5 MHz, 10 W cm^{-2}, 10% duty cycle, 330 s	SCC7 cells	31
	α-Fe_2O_3@Pt	1.0 MHz, 1.0 W cm^{-2}, 3 min	4T1 cells	32
	Fe–VS_2-PEG	40 kHz, 4.5 W cm^{-2}, 5 min	4T1 cells	113
Transition metal oxide nanomaterials	$MnWO_x$-PEG	40 kHz, 3 W cm^{-2}, 5 min, 50% duty cycle	4T1 cells	33
	Fe–TiO_2-PEG	40 kHz, 3 W cm^{-2}, 33% duty cycle, 15 min	4T1 cells	34
Carbon-based nanomaterials	C-doped TiO_2	1.0 MHz, 1.8 W cm^{-2}, 50% duty cycle, 90 s	4T1 cells	37
	MnO_x/TiO_2-GR	1.0 MHz, 1.5 W cm^{-2}, 50% duty cycle, 60 s	4T1 cells	38
	Pt/N-CD@TiO_{2-x}	50 kHz, 2.0 W cm^{-2}, 5 min	143B cells	39
Mn-based nanomaterials	Zr-MOF@AIPH	1 MHz, 1.0 W cm^{-2}, 1 min	PancO2 cells	45
	PMCS	1.0 MHz, 1.5 W cm^{-2}, 1 min	4T1 cells	46
	Mn-MOF	1 MHz, 1.0 W cm^{-2}, 50% duty cycle, 5 min	H22 cells, 4T1 cells	47
	Cu-MOF/Ce6	2.0 W cm^{-2}, 10 min	MCF-7 cells	114

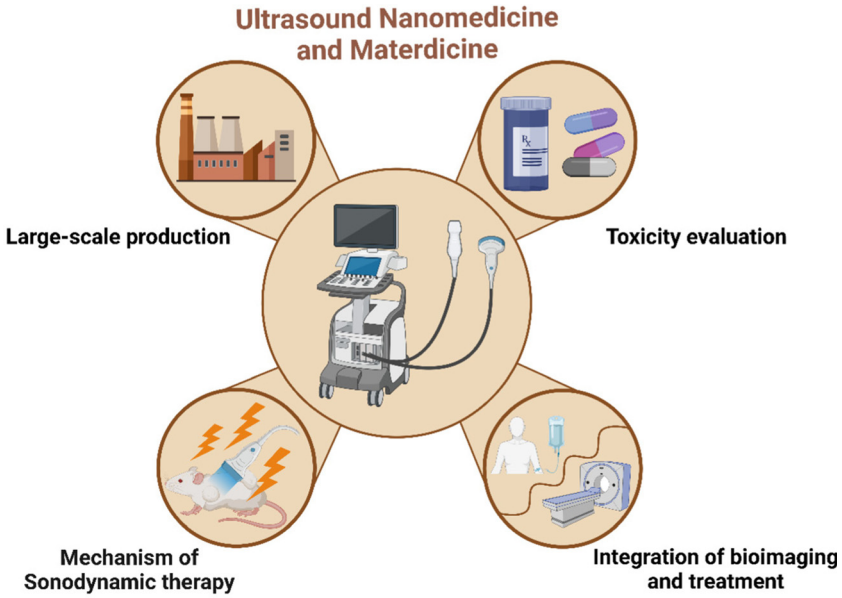

Fig. 15 Schematic illustration of the development and challenges of ultrasound nanomedicine and materdicine, including large-scale production, toxicity evaluation, US-related therapeutic mechanisms, integration of bioimaging and treatment.

sonosensitizers is a research hotspot in various disciplines of ultrasonic diagnosis and treatment. MBs, polymer NPs, lipid vesicles and inorganic NPs (including gold, titanium dioxide, carbon, and silicon dioxide NPs) have been proved to be desirable sonosensitizers. This review comprehensively summarized the research progress of various sonosensitizers based on the development of nanomedicine and materdicine, especially the nanosonosensitizers in ultrasonic diagnosis and treatment in recent years (Table 1). In addition, we also focus on the latest research progress of different diagnosis and treatment modalities of sonosensitizers, including SDT combined with chemotherapy, immunotherapy, PDT, PTT and gas therapy. Furthermore, US-related therapeutic mechanisms including cavitation, ROS generation and apoptosis have been discussed in detail. The development of sonosensitizers provides a new research direction for traditional ultrasonic diagnosis and treatment. However, many studies are still in the early development stages and further exhaustive research is still highly required to confirm the therapeutic efficiency and biosafety. How to translate basic research into clinical practice, lessen patient suffering, and enhance illness prognosis still faces some significant hurdles, as listed in the following several sections (Fig. 15).

(1) Controllable preparation and mass production. One of the key factors for the successful conversion of sonosensitizers is to control the preparation process of nanomedicines and biomaterials and retain their physical and chemical properties, including morphology, size, surface chemistry and composition. At the same time, the preparation repeatability should be considered to ensure the sustainability of follow-up diagnosis and treatment. Based on this point, the standardized preparation methods should be explored to control the synthetic process of different sonosensitizers. In addition, the main issues to be resolved in large-scale production and clinical transformation are lowering the cost of production and streamlining the preparation process.

(2) Toxicity evaluation. The toxic side effects of sonosensitizers on normal cells and animal models are insufficient. Hence, the key to promoting sonosensitizers' clinical testing and even clinical transformation is thoroughly assessing the biocompatibility and biosafety of sonosensitizers both *in vitro* and *in vivo*, as well as determining the most suitable dose, exposure time, administration route, and frequency of sonosensitizers. In addition, animal models (such as mouse) used in biomedical evaluation may not be able to fully simulate the complex human body microenvironment. Therefore, the large animals or even non-human primates is essential to evaluate the toxicity of the engineered sonosensitizers.

(3) Biological barrier. The potential mechanisms of SDT in inhibiting tumor metastasis and bacterial infection are still controversial. Comprehensive understanding of the exact mechanism of SDT will guide the design of sonosensitizers with the desirable therapeutic effect, which provides solid theoretical foundation for future practical SDT-related treatment.

(4) Integration of bioimaging and treatment. One of the design purposes of the application of sonosensitizers in ultrasonic medicine is to achieve the integration of bioimaging and treatment through a single agent. However, there are very few promising examples of accurate and real-time monitoring of treatment progress. Real time multimodal imaging monitoring can provide accurate information and guide the therapeutic process for disease localization and reflect important information such as pharmacokinetics, biological distribution and metabolism of sonosensitizers, thus providing guidance for further treatment. Therefore, the development of a new kind of highly effective sonosensitizers that can be utilized for both

bioimaging and therapy, while maximizing the theranostic performance is highly crucial for the development of ultrasonic medicine in the near future.

In summary, US-related diagnosis and treatment of different diseases could be dramatically altered by the burgeoning fields of nanomedicine and materdicine, which requires the cooperation of researchers and scientists with different disciplinary backgrounds, thereby jointly promoting the development of US nanomedicine and materdicine for further clinical translation and benefiting the patients.

Conflicts of interest

There are no conflicts to declare.

Acknowledgements

This work was financially supported by the National Science Foundation for Young Scientists of China (Grant No. 52002390), Shanghai Science and Technology Program (Grant No. 21010500100, 22140901700, 22DZ2204700, and 22142202200), the Basic Research Program of Shanghai Municipal Government (Grant No. 21JC1406002) and Shanghai Shuguang Program (Grant No. 21SG39).

References

1 B. Y. Kim, J. T. Rutka and W. C. Chan, Nanomedicine, *N. Engl. J. Med.*, 2010, **363**(25), 2434–2443.
2 J. Son, *et al.*, Light-responsive nanomedicine for biophotonic imaging and targeted therapy, *Adv. Drug Delivery Rev.*, 2019, **138**, 133–147.
3 S. Snipstad, *et al.*, Ultrasound and microbubbles to beat barriers in tumors: Improving delivery of nanomedicine, *Adv. Drug Delivery Rev.*, 2021, **177**, 113847.
4 I. T. Smith, *et al.*, Nanomedicine and nanobiotechnology applications of magnetoelectric nanoparticles, *Wiley Interdiscip. Rev.: Nanomed. Nanobiotechnol.*, 2022, e1849.
5 K. Wu, *et al.*, Magnetic nanoparticles in nanomedicine: a review of recent advances, *Nanotechnology*, 2019, **30**(50), 502003.
6 V. S. Bachu, *et al.*, High-Intensity Focused Ultrasound: A Review of Mechanisms and Clinical Applications, *Ann. Biomed. Eng.*, 2021, **49**(9), 1975–1991.
7 Y. Liu, *et al.*, Nanobiomaterials: from 0D to 3D for tumor therapy and tissue regeneration, *Nanoscale*, 2019, **11**(29), 13678–13708.
8 S. Son, *et al.*, Multifunctional sonosensitizers in sonodynamic cancer therapy, *Chem. Soc. Rev.*, 2020, **49**(11), 3244–3261.
9 P. Geng, *et al.*, Sub 5 nm Gd(3+)-Hemoporfin Framework Nanodots for Augmented Sonodynamic Theranostics and Fast Renal Clearance, *Adv. Healthcare Mater.*, 2021, **10**(18), e2100703.
10 D. Sun, *et al.*, Ultrasound-Switchable Nanozyme Augments Sonodynamic Therapy against Multidrug-Resistant Bacterial Infection, *ACS Nano*, 2020, **14**(2), 2063–2076.
11 M. Wen, *et al.*, On-demand assembly of polymeric nanoparticles for longer-blood-circulation and disassembly in tumor for boosting sonodynamic therapy, *Bioact. Mater.*, 2022, **18**, 242–253.
12 P. Zhao, *et al.*, Nanoparticle-Assisted Sonosensitizers and Their Biomedical Applications, *Int. J. Nanomed.*, 2021, **16**, 4615–4630.
13 C. Hu, B. Hou and S. Xie, Application of nanosonosensitizer materials in cancer sono-dynamic therapy, *RSC Adv.*, 2022, **12**(35), 22722–22747.
14 Z. Gong and Z. Dai, Design and Challenges of Sonodynamic Therapy System for Cancer Theranostics: From Equipment to Sensitizers, *Adv. Sci.*, 2021, **8**(10), 2002178.
15 S. Umemura, *et al.*, Mechanism of cell damage by ultrasound in combination with hematoporphyrin, *Jpn. J. Cancer Res.*, 1990, **81**(9), 962–966.
16 K. Bilmin, T. Kujawska and P. Grieb, Sonodynamic Therapy for Gliomas. Perspectives and Prospects of Selective Sonosensitization of Glioma Cells, *Cells*, 2019, **8**(11), 1428.
17 X. B. Wang, *et al.*, Study of cell killing effect on S180 by ultrasound activating protoporphyrin IX, *Ultrasonics*, 2008, **48**(2), 135–140.
18 H. Jin, *et al.*, Sonodynamic effects of hematoporphyrin monomethyl ether on CNE-2 cells detected by atomic force microscopy, *J. Cell. Biochem.*, 2011, **112**(1), 169–178.
19 Z. Tian, *et al.*, Hematoporphyrin monomethyl ether enhances the killing of ultrasound on osteosarcoma cells involving intracellular reactive oxygen species and calcium ion elevation, *Integr. Cancer Ther.*, 2010, **9**(4), 365–369.
20 K. Milowska and T. Gabryelak, Synergistic effect of ultrasound and phthalocyanines on nucleated erythrocytes *in vitro*, *Ultrasound Med. Biol.*, 2005, **31**(12), 1707–1712.
21 M. Maia, *et al.*, Xanthenes in Medicinal Chemistry - Synthetic strategies and biological activities, *Eur. J. Med. Chem.*, 2021, **210**, 113085.
22 Z. Y. Yu, *et al.*, Rose bengal as photocatalyst: visible light-mediated Friedel-Crafts alkylation of indoles with nitroalkenes in water, *RSC Adv.*, 2020, **10**(8), 4825–4831.
23 S. Umemura, *et al.*, Sonodynamically induced effect of rose bengal on isolated sarcoma 180 cells, *Cancer Chemother. Pharmacol.*, 1999, **43**(5), 389–393.
24 T. Yoshida, *et al.*, Combination of doxorubicin and low-intensity ultrasound causes a synergistic enhancement in cell killing and an additive enhancement in apoptosis induction in human lymphoma U937 cells, *Cancer Chemother. Pharmacol.*, 2008, **61**(4), 559–567.
25 F. Grande and P. Tucci, Titanium Dioxide Nanoparticles: a Risk for Human Health?, *Mini-Rev. Med. Chem.*, 2016, **16**(9), 762–769.
26 Y. Harada, *et al.*, Ultrasound activation of TiO_2 in melanoma tumors, *J. Controlled Release*, 2011, **149**(2), 190–195.

27 X. Wang, *et al.*, Ultrafine Titanium Monoxide (TiO(1 + *x*)) Nanorods for Enhanced Sonodynamic Therapy, *J. Am. Chem. Soc.*, 2020, **142**(14), 6527–6537.
28 B. Geng, *et al.*, W-Doped TiO(2) Nanorods for Multimode Tumor Eradication in Osteosarcoma Models under Single Ultrasound Irradiation, *ACS Appl. Mater. Interfaces*, 2021, **13**(38), 45325–45334.
29 K. Ninomiya, *et al.*, Targeted sonocatalytic cancer cell injury using avidin-conjugated titanium dioxide nanoparticles, *Ultrason. Sonochem.*, 2014, **21**(5), 1624–1628.
30 Y. Zhu, *et al.*, Rapid bacterial elimination achieved by sonodynamic Au@Cu(2)O hybrid nanocubes, *Nanoscale*, 2021, **13**(37), 15699–15710.
31 V. G. Deepagan, *et al.*, Long-Circulating Au–TiO(2) Nanocomposite as a Sonosensitizer for ROS-Mediated Eradication of Cancer, *Nano Lett.*, 2016, **16**(10), 6257–6264.
32 T. Zhang, *et al.*, α-Fe(2)O(3)@Pt heterostructure particles to enable sonodynamic therapy with self-supplied O(2) and imaging-guidance, *J. Nanobiotechnol.*, 2021, **19**(1), 358.
33 F. Gong, *et al.*, Ultrasmall Oxygen-Deficient Bimetallic Oxide MnWO(X) Nanoparticles for Depletion of Endogenous GSH and Enhanced Sonodynamic Cancer Therapy, *Adv. Mater.*, 2019, **31**(23), e1900730.
34 S. Bai, *et al.*, Ultrasmall Iron-Doped Titanium Oxide Nanodots for Enhanced Sonodynamic and Chemodynamic Cancer Therapy, *ACS Nano*, 2020, **14**(11), 15119–15130.
35 H. Liu, *et al.*, Carbon-Based Nanomaterials for Bone and Cartilage Regeneration: A Review, *ACS Biomater. Sci. Eng.*, 2021, **7**(10), 4718–4735.
36 S. H. Ku, M. Lee and C. B. Park, Carbon-based nanomaterials for tissue engineering, *Adv. Healthcare Mater.*, 2013, **2**(2), 244–260.
37 C. C. Yang, *et al.*, Using C-doped TiO(2) Nanoparticles as a Novel Sonosensitizer for Cancer Treatment, *Antioxidants*, 2020, (9), 9.
38 C. Dai, *et al.*, Two-Dimensional Graphene Augments Nanosonosensitized Sonocatalytic Tumor Eradication, *ACS Nano*, 2017, **11**(9), 9467–9480.
39 B. Geng, *et al.*, Platinum Crosslinked Carbon Dot@TiO(2-)(x) p-n Junctions for Relapse-Free Sonodynamic Tumor Eradication via High-Yield ROS and GSH Depletion, *Small*, 2022, **18**(6), e2103528.
40 Y. Li, *et al.*, Synthesis and shaping of metal-organic frameworks: a review, *Chem. Commun.*, 2022, **58**(82), 11488–11506.
41 L. Yang, *et al.*, Tirapazamine-loaded UiO-66/Cu for ultrasound-mediated promotion of chemodynamic therapy cascade hypoxia-activated anticancer therapy, *J. Colloid Interface Sci.*, 2022, **634**, 495–508.
42 Q. Zhang, *et al.*, A biotin-stabilized HKUST-1/ADM scaffold for facilitating MSC endothelial differentiation and vascularization in diabetic wound healing, *Biomater. Sci.*, 2023, **11**, 854–872.
43 X. G. Yang, *et al.*, Enhanced Activity of Enzyme Immobilized on Hydrophobic ZIF-8 Modified by Ni^{2+} Ions, *Angew. Chem., Int. Ed.*, 2023, **62**(7), e202216699.
44 L. Guo, *et al.*, A Novel Signal-On Electrochemiluminescence Immunosensor for the Detection of NSCLC Antigen Biomarker Based on New Co-Reaction Accelerators, *Adv. Healthcare Mater.*, 2022, e2202287.
45 C. Zhang, *et al.*, Metal-Organic Framework (MOF)-Based Ultrasound-Responsive Dual-Sonosensitizer Nanoplatform for Hypoxic Cancer Therapy, *Adv. Healthcare Mater.*, 2022, **11**(2), e2101946.
46 X. Pan, *et al.*, Metal-Organic-Framework-Derived Carbon Nanostructure Augmented Sonodynamic Cancer Therapy, *Adv. Mater.*, 2018, **30**(23), e1800180.
47 Q. Xu, *et al.*, Manganese porphyrin-based metal-organic framework for synergistic sonodynamic therapy and ferroptosis in hypoxic tumors, *Theranostics*, 2021, **11**(4), 1937–1952.
48 J. Ouyang, *et al.*, Minimally invasive nanomedicine: nanotechnology in photo-/ultrasound-/radiation-/magnetism-mediated therapy and imaging, *Chem. Soc. Rev.*, 2022, **51**(12), 4996–5041.
49 N. Deshpande, A. Needles and J. K. Willmann, Molecular ultrasound imaging: current status and future directions, *Clin. Radiol.*, 2010, **65**(7), 567–581.
50 J. Mu, *et al.*, Development of endogenous enzyme-responsive nanomaterials for theranostics, *Chem. Soc. Rev.*, 2018, **47**(15), 5554–5573.
51 L. Tu, *et al.*, Ultrasound-controlled drug release and drug activation for cancer therapy, *Exploration*, 2021, **1**(3), 20210023.
52 J. Zhang, L. Wei and Y. Zhao, Synthesis of nanobubbles for improved ultrasound tumor-imaging applications, *3 Biotech.*, 2020, **10**(1), 12.
53 D. R. Spahn, Blood substitutes. Artificial oxygen carriers: perfluorocarbon emulsions, *Crit. Care*, 1999, **3**(5), R93–R97.
54 G. M. Lanza, *et al.*, A novel site-targeted ultrasonic contrast agent with broad biomedical application, *Circulation*, 1996, **94**(12), 3334–3340.
55 K. Loskutova, D. Grishenkov and M. Ghorbani, Review on Acoustic Droplet Vaporization in Ultrasound Diagnostics and Therapeutics, *BioMed Res. Int.*, 2019, **2019**, 9480193.
56 J. Zhu, *et al.*, Polydopamine-Encapsulated Perfluorocarbon for Ultrasound Contrast Imaging and Photothermal Therapy, *Mol. Pharmaceutics*, 2020, **17**(3), 817–826.
57 F. Chen, *et al.*, Exosome-like silica nanoparticles: a novel ultrasound contrast agent for stem cell imaging, *Nanoscale*, 2017, **9**(1), 402–411.
58 M. Kuniyil Ajith Singh and W. Xia, Biomedical Photoacoustic Imaging and Sensing Using Affordable Resources, *Sensors*, 2021, **21**(7), 2572.
59 A. B. E. Attia, *et al.*, A review of clinical photoacoustic imaging: Current and future trends, *Photoacoustics*, 2019, **16**, 100144.
60 E. Jung, *et al.*, Molecularly Engineered Theranostic Nanoparticles for Thrombosed Vessels: H(2)O(2)-Activatable Contrast-Enhanced Photoacoustic Imaging and Antithrombotic Therapy, *ACS Nano*, 2018, **12**(1), 392–401.
61 G. Shapiro, *et al.*, Multiparameter evaluation of in vivo gene delivery using ultrasound-guided, microbubble-enhanced sonoporation, *J. Controlled Release*, 2016, **223**, 157–164.

62 X. Cai, *et al.*, Ultrasound-Responsive Materials for Drug/Gene Delivery, *Front. Pharmacol.*, 2019, **10**, 1650.
63 L. Duan, *et al.*, Micro/nano-bubble-assisted ultrasound to enhance the EPR effect and potential theranostic applications, *Theranostics*, 2020, **10**(2), 462–483.
64 F. Yan, *et al.*, Paclitaxel-liposome-microbubble complexes as ultrasound-triggered therapeutic drug delivery carriers, *J. Controlled Release*, 2013, **166**(3), 246–255.
65 E. G. Schutt, *et al.*, Injectable microbubbles as contrast agents for diagnostic ultrasound imaging: the key role of perfluorochemicals, *Angew. Chem., Int. Ed.*, 2003, **42**(28), 3218–3235.
66 L. Zhang, *et al.*, Size-Modulable Nanoprobe for High-Performance Ultrasound Imaging and Drug Delivery against Cancer, *ACS Nano*, 2018, **12**(4), 3449–3460.
67 C. Zhou, *et al.*, Novel Class of Ultrasound-Triggerable Drug Delivery Systems for the Improved Treatment of Tumors, *Mol. Pharmaceutics*, 2019, **16**(7), 2956–2965.
68 S. Kotopoulis, *et al.*, Treatment of human pancreatic cancer using combined ultrasound, microbubbles, and gemcitabine: a clinical case study, *Med. Phys.*, 2013, **40**(7), 072902.
69 J. Sitta and C. M. Howard, Applications of Ultrasound-Mediated Drug Delivery and Gene Therapy, *Int. J. Mol. Sci.*, 2021, **22**(21), 11491.
70 Y. Liu, *et al.*, Synergistic anti-tumor effect of anti-PD-L1 antibody cationic microbubbles for delivery of the miR-34a gene combined with ultrasound on cervical carcinoma, *Am. J. Transl. Res.*, 2021, **13**(3), 988–1005.
71 R. Suzuki, *et al.*, Novel dianostics and therapeutics with ultrasound technologies and nanotechnologies, *Yakugaku Zasshi*, 2013, **133**(12), 1263–1268.
72 J. R. Lindner, *et al.*, Microvascular rheology of Definity microbubbles after intra-arterial and intravenous administration, *J. Am. Soc. Echocardiogr.*, 2002, **15**(5), 396–403.
73 Y. Watanabe, *et al.*, Delivery of Na/I symporter gene into skeletal muscle using nanobubbles and ultrasound: visualization of gene expression by PET, *J. Nucl. Med.*, 2010, **51**(6), 951–958.
74 W. Cai, *et al.*, The therapeutic effect in gliomas of nanobubbles carrying siRNA combined with ultrasound-targeted destruction, *Int. J. Nanomed.*, 2018, **13**, 6791–6807.
75 Y. C. Chen, *et al.*, Pluronic block copolymers: novel functions in ultrasound-mediated gene transfer and against cell damage, *Ultrasound Med. Biol.*, 2006, **32**(1), 131–137.
76 F. Orsi, *et al.*, High intensity focused ultrasound ablation: a new therapeutic option for solid tumors, *J. Cancer Res. Ther.*, 2010, **6**(4), 414–420.
77 T. Yamaguchi, *et al.*, Current Landscape of Sonodynamic Therapy for Treating Cancer, *Cancers*, 2021, (24), 13.
78 G. Canavese, *et al.*, Nanoparticle-assisted ultrasound: A special focus on sonodynamic therapy against cancer, *Chem. Eng. J.*, 2018, **340**, 155–172.
79 F. Wu, High intensity focused ultrasound: a noninvasive therapy for locally advanced pancreatic cancer, *World J. Gastroenterol.*, 2014, **20**(44), 16480–16488.
80 G. T. Clement, Perspectives in clinical uses of high-intensity focused ultrasound, *Ultrasonics*, 2004, **42**(10), 1087–1093.
81 Y. F. Zhou, High intensity focused ultrasound in clinical tumor ablation, *World J. Clin. Oncol.*, 2011, **2**(1), 8–27.
82 J. Kim, *et al.*, Therapeutic effect of high-intensity focused ultrasound combined with transarterial chemoembolisation for hepatocellular carcinoma <5 cm: comparison with transarterial chemoembolisation monotherapy-preliminary observations, *Br. J. Radiol.*, 2012, **85**(1018), e940–e946.
83 W. Luo, *et al.*, Enhancement of ultrasound contrast agent in high-intensity focused ultrasound ablation, *Adv. Ther.*, 2006, **23**(6), 861–868.
84 M. H. Yu, *et al.*, Therapeutic Effects of Microbubbles Added to Combined High-Intensity Focused Ultrasound and Chemotherapy in a Pancreatic Cancer Xenograft Model, *Korean J. Radiol.*, 2016, **17**(5), 779–788.
85 L. C. Moyer, *et al.*, High-intensity focused ultrasound ablation enhancement in vivo via phase-shift nanodroplets compared to microbubbles, *J. Ther. Ultrasound*, 2015, **3**, 7.
86 H. Han, *et al.*, Effect of high intensity focused ultrasound (HIFU) in conjunction with a nanomedicines-microbubble complex for enhanced drug delivery, *J. Controlled Release*, 2017, **266**, 75–86.
87 Y. You, *et al.*, Nanoparticle-enhanced synergistic HIFU ablation and transarterial chemoembolization for efficient cancer therapy, *Nanoscale*, 2016, **8**(7), 4324–4339.
88 C. Yang, *et al.*, Recent advances in ultrasound-triggered therapy, *J. Drug Targeting*, 2019, **27**(1), 33–50.
89 D. Costley, *et al.*, Treating cancer with sonodynamic therapy: a review, *Int. J. Hyperthermia*, 2015, **31**(2), 107–117.
90 G. Y. Wan, *et al.*, Recent advances of sonodynamic therapy in cancer treatment, *Cancer Biol. Med.*, 2016, **13**(3), 325–338.
91 Y. Si, *et al.*, Phase-Transformation Nanoparticle-Mediated Sonodynamic Therapy: An Effective Modality to Enhance Anti-Tumor Immune Response by Inducing Immunogenic Cell Death in Breast Cancer, *Int. J. Nanomed.*, 2021, **16**, 1913–1926.
92 H. Zhao, *et al.*, Biomimetic Decoy Inhibits Tumor Growth and Lung Metastasis by Reversing the Drawbacks of Sonodynamic Therapy, *Adv. Healthcare Mater.*, 2020, **9**(1), e1901335.
93 X. Qian, X. Han and Y. Chen, Insights into the unique functionality of inorganic micro/nanoparticles for versatile ultrasound theranostics, *Biomaterials*, 2017, **142**, 13–30.
94 X. Ji, *et al.*, Capturing functional two-dimensional nanosheets from sandwich-structure vermiculite for cancer theranostics, *Nat. Commun.*, 2021, **12**(1), 1124.
95 C. Münch and I. Dikic, Hitchhiking on selective autophagy, *Nat. Cell Biol.*, 2018, **20**(2), 122–124.
96 L. Zhou, *et al.*, Autophagy blockade synergistically enhances nanosonosensitizer-enabled sonodynamic cancer nanotherapeutics, *J. Nanobiotechnol.*, 2021, **19**(1), 112.

97 R. Y. Zhang, *et al.*, A pH/ultrasonic dual-response step-targeting enterosoluble granule for combined sonodynamic-chemotherapy guided via gastrointestinal tract imaging in orthotopic colorectal cancer, *Nanoscale*, 2021, **13**(7), 4278–4294.
98 X. He and C. Xu, Immune checkpoint signaling and cancer immunotherapy, *Cell Res.*, 2020, **30**(8), 660–669.
99 W. Yue, *et al.*, Checkpoint blockade and nanosonosensitizer-augmented noninvasive sonodynamic therapy combination reduces tumour growth and metastases in mice, *Nat. Commun.*, 2019, **10**(1), 2025.
100 S. Chen, *et al.*, Multi-Modal Imaging Monitored M2 Macrophage Targeting Sono-Responsive Nanoparticles to Combat MRSA Deep Infections, *Int. J. Nanomed.*, 2022, **17**, 4525–4546.
101 L. Rengeng, *et al.*, Sonodynamic therapy, a treatment developing from photodynamic therapy, *Photodiagn. Photodyn. Ther.*, 2017, **19**, 159–166.
102 Y. Liu, *et al.*, Sinoporphyrin sodium triggered sonophotodynamic effects on breast cancer both *in vitro* and in vivo, *Ultrason. Sonochem.*, 2016, **31**, 437–448.
103 R. W. Redmond and I. E. Kochevar, Medical Applications of Rose Bengal- and Riboflavin-Photosensitized Protein Crosslinking, *Photochem. Photobiol.*, 2019, **95**(5), 1097–1115.
104 H. J. Chen, *et al.*, Synthesis and biological characterization of novel rose bengal derivatives with improved amphiphilicity for sono-photodynamic therapy, *Eur. J. Med. Chem.*, 2018, **145**, 86–95.
105 S. Liang, *et al.*, Intelligent Hollow Pt-CuS Janus Architecture for Synergistic Catalysis-Enhanced Sonodynamic and Photothermal Cancer Therapy, *Nano Lett.*, 2019, **19**(6), 4134–4145.
106 G. Li, *et al.*, Titanium carbide nanosheets with defect structure for photothermal-enhanced sonodynamic therapy, *Bioact. Mater.*, 2022, **8**, 409–419.
107 X. Wang, *et al.*, Recent progress of chemodynamic therapy-induced combination cancer therapy, *Nano Today*, 2020, **35**, 100946.
108 B. Yang, Y. Chen and J. Shi, Reactive Oxygen Species (ROS)-Based Nanomedicine, *Chem. Rev.*, 2019, **119**(8), 4881–4985.
109 Z. Tang, *et al.*, Chemodynamic Therapy: Tumour Microenvironment-Mediated Fenton and Fenton-like Reactions, *Angew. Chem., Int. Ed.*, 2019, **58**(4), 946–956.
110 C. Dong, *et al.*, The Coppery Age: Copper (Cu)-Involved Nanotheranostics, *Adv. Sci.*, 2020, **7**(21), 2001549.
111 Y. N. Hao, *et al.*, State-of-the-art advances of copper-based nanostructures in the enhancement of chemodynamic therapy, *J. Mater. Chem. B*, 2021, **9**(2), 250–266.
112 C. Liu, *et al.*, An open source and reduce expenditure ROS generation strategy for chemodynamic/photodynamic synergistic therapy, *Nat. Commun.*, 2020, **11**(1), 1735.
113 H. Lei, *et al.*, Biodegradable Fe-Doped Vanadium Disulfide Theranostic Nanosheets for Enhanced Sonodynamic/Chemodynamic Therapy, *ACS Appl. Mater. Interfaces*, 2020, **12**(47), 52370–52382.
114 K. Zhang, *et al.*, Enhanced cancer therapy by hypoxia-responsive copper metal-organic frameworks nanosystem, *Biomaterials*, 2020, **258**, 120278.
115 Y. Yu, *et al.*, Progress and prospects of nanozymes for enhanced antitumor therapy, *Front. Chem.*, 2022, **10**, 1090795.
116 X. Wang, *et al.*, Progress and perspectives of platinum nanozyme in cancer therapy, *Front. Chem.*, 2022, **10**, 1092747.
117 Q. Wang, J. Jiang and L. Gao, Nanozyme-based medicine for enzymatic therapy: progress and challenges, *Biomed. Mater.*, 2021, **16**(4), 042002.
118 N. Tao, *et al.*, A Cascade Nanozyme with Amplified Sonodynamic Therapeutic Effects through Comodulation of Hypoxia and Immunosuppression against Cancer, *ACS Nano*, 2022, **16**(1), 485–501.
119 Y. Opoku-Damoah, *et al.*, Therapeutic gas-releasing nanomedicines with controlled release: Advances and perspectives, *Exploration*, 2022, **2**(5), 20210181.
120 J. Yan, *et al.*, The Advancement of Gas-Generating Nanoplatforms in Biomedical Fields: Current Frontiers and Future Perspectives, *Small Methods*, 2022, **6**(7), 2200139.
121 R. M. Pascale, *et al.*, The Warburg Effect 97 Years after Its Discovery, *Cancers*, 2020, (10), 12.
122 L. Chen, *et al.*, Gas-Mediated Cancer Bioimaging and Therapy, *ACS Nano*, 2019, **13**(10), 10887–10917.
123 S. Zuo, *et al.*, Mitochondria-Targeted Mesoporous Titanium Dioxide Nanoplatform for Synergistic Nitric Oxide Gas-Sonodynamic Therapy of Breast Cancer, *Int. J. Nanomed.*, 2022, **17**, 989–1002.
124 Y. Liu, *et al.*, Magnetic Nanoliposomes as in Situ Microbubble Bombers for Multimodality Image-Guided Cancer Theranostics, *ACS Nano*, 2017, **11**(2), 1509–1519.
125 L. A. Crum and R. A. Roy, Sonoluminescence, *Science*, 1994, **266**(5183), 233–234.
126 R. Hiller, S. J. Putterman and B. P. Barber, Spectrum of synchronous picosecond sonoluminescence, *Phys. Rev. Lett.*, 1992, **69**(8), 1182–1184.
127 E. Beguin, *et al.*, Direct Evidence of Multibubble Sonoluminescence Using Therapeutic Ultrasound and Microbubbles, *ACS Appl. Mater. Interfaces*, 2019, **11**(22), 19913–19919.
128 Y. T. Didenko and K. S. Suslick, The energy efficiency of formation of photons, radicals and ions during single-bubble cavitation, *Nature*, 2002, **418**(6896), 394–397.
129 K. Logan, *et al.*, Targeted chemo-sonodynamic therapy treatment of breast tumours using ultrasound responsive microbubbles loaded with paclitaxel, doxorubicin and Rose Bengal, *Eur. J. Pharm. Biopharm.*, 2019, **139**, 224–231.
130 S. Kwon, *et al.*, Nanomedicines for Reactive Oxygen Species Mediated Approach: An Emerging Paradigm for Cancer Treatment, *Acc. Chem. Res.*, 2019, **52**(7), 1771–1782.
131 Y. Li, *et al.*, IR-780 Dye as a Sonosensitizer for Sonodynamic Therapy of Breast Tumor, *Sci. Rep.*, 2016, **6**, 25968.
132 P. M. Winter *et al.*, Piezoelectric Effect at Nanoscale, *Encyclopedia of Nanotechnology*, 2012.
133 M. T. Chorsi, *et al.*, Piezoelectric Biomaterials for Sensors and Actuators, *Adv. Mater.*, 2019, **31**(1), e1802084.
134 Y. Dong, *et al.*, 2D Piezoelectric Bi(2) MoO(6) Nanoribbons for GSH-Enhanced Sonodynamic Therapy, *Adv. Mater.*, 2021, **33**(51), e2106838.

135 S. Masimukku, *et al.*, High Efficient Degradation of Dye Molecules by PDMS Embedded Abundant Single-layer Tungsten Disulfide and Their Antibacterial Performance, *Nano Energy*, 2018, **46**, 338–346.
136 Y. F. Li and Z. P. Liu, Particle size, shape and activity for photocatalysis on titania anatase nanoparticles in aqueous surroundings, *J. Am. Chem. Soc.*, 2011, **133**(39), 15743–15752.
137 X. Wang, *et al.*, Direct-current nanogenerator driven by ultrasonic waves, *Science*, 2007, **316**(5821), 102–105.
138 Y. Nosaka and A. Y. Nosaka, Generation and Detection of Reactive Oxygen Species in Photocatalysis, *Chem. Rev.*, 2017, **117**(17), 11302–11336.
139 J. Wu, *et al.*, Strong pyro-catalysis of pyroelectric $BiFeO_3$ nanoparticles under a room-temperature cold-hot alternation, *Nanoscale*, 2016, **8**(13), 7343–7350.
140 Y. Wang, *et al.*, Piezo-catalysis for nondestructive tooth whitening, *Nat. Commun.*, 2020, **11**(1), 1328.
141 X. Wang, *et al.*, Initiation of autophagy and apoptosis by sonodynamic therapy in murine leukemia L1210 cells, *Toxicol. In Vitro*, 2013, **27**(4), 1247–1259.
142 L. Lagneaux, *et al.*, Ultrasonic low-energy treatment: a novel approach to induce apoptosis in human leukemic cells, *Exp. Hematol.*, 2002, **30**(11), 1293–1301.
143 E. Li, *et al.*, Sinoporphyrin sodium based sonodynamic therapy induces anti-tumor effects in hepatocellular carcinoma and activates p53/caspase 3 axis, *Int. J. Biochem. Cell Biol.*, 2019, **113**, 104–114.
144 S. Dai, *et al.*, *In vitro* stimulation of calcium overload and apoptosis by sonodynamic therapy combined with hematoporphyrin monomethyl ether in C6 glioma cells, *Oncol. Lett.*, 2014, **8**(4), 1675–1681.